Supplementary Information

Thermally Activated Delayed Fluorescence Emitters for Efficient Sensitization of Europium (III)

Neena K Kalluvettukuzhy, Michal R Maciejczyk, Neil Robertson*
EaStCHEM School of Chemistry
University of Edinburgh
Kings Buildings, Edinburgh EH9 3FJ, U.K
E-mail: Neil.Robertson@ed.ac.uk

Table of Contents

Table S1: Comparison of the ^{19}F and ^{31}P chemical shift values of ligands and complexes

Ligands			Complex		
	^{19}F δ (ppm)	^{31}P δ (ppm)		^{19}F δ (ppm)	^{31}P δ (ppm)
tta	-75.7	**-**	**$Eutta_3.2H_2O$**	-82.3	-
1L	-	28.38 – 28.26 (m)	**1**	-79.7	-76.5
2L	-	28.37 – 28.52 (m)	**2**	-79.5	-76.3
3L	-	28.58 – 28.43 (m)	**3**	-79.5	-75.9

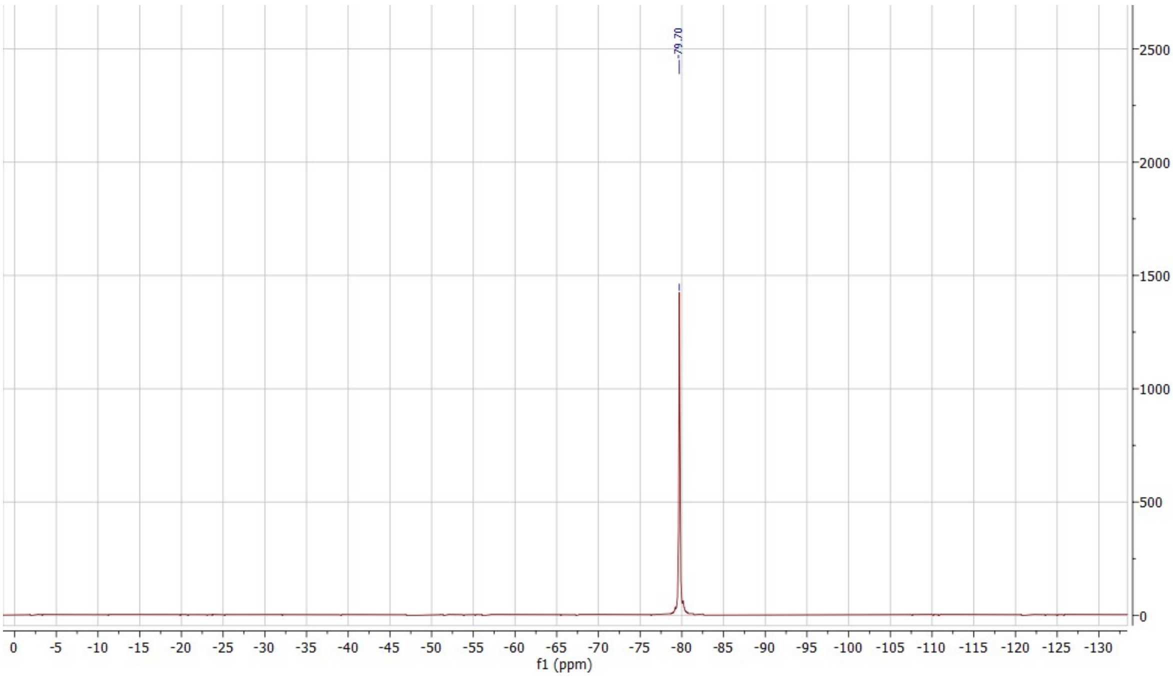

Figure S1. ^{19}F NMR spectra of Eu(III) coordination polymer **1** in C_6D_6 at 25 °C

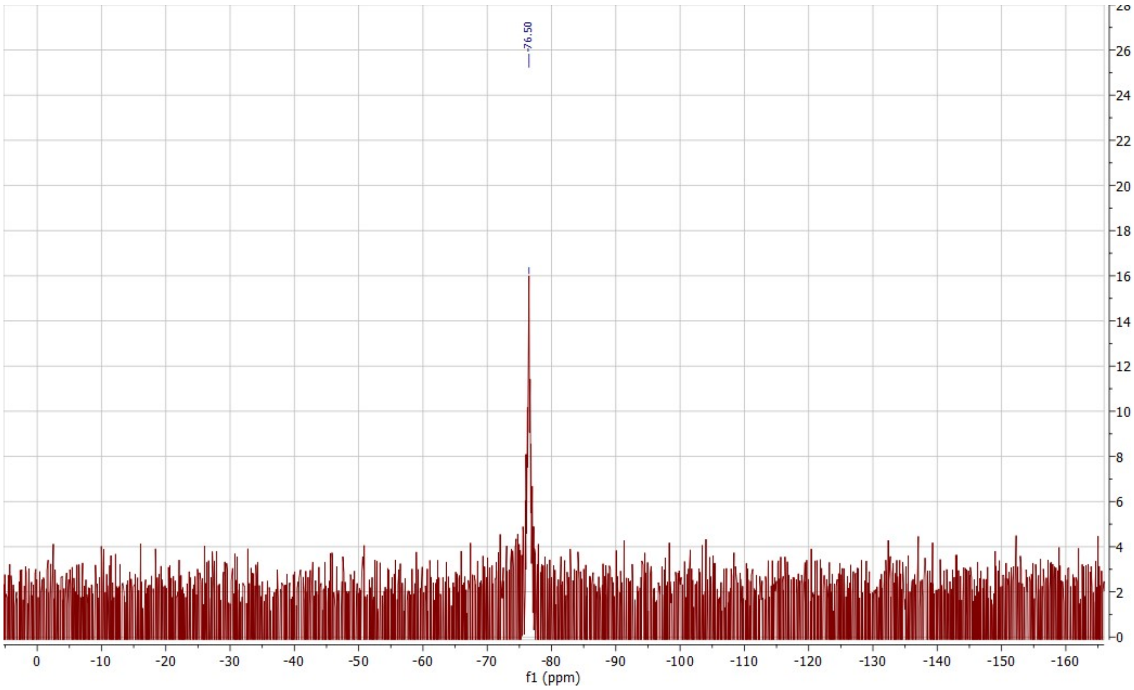

Figure S2. [31]P NMR spectra of Eu (III) coordination polymer **1** in C_6D_6 at 25 °C

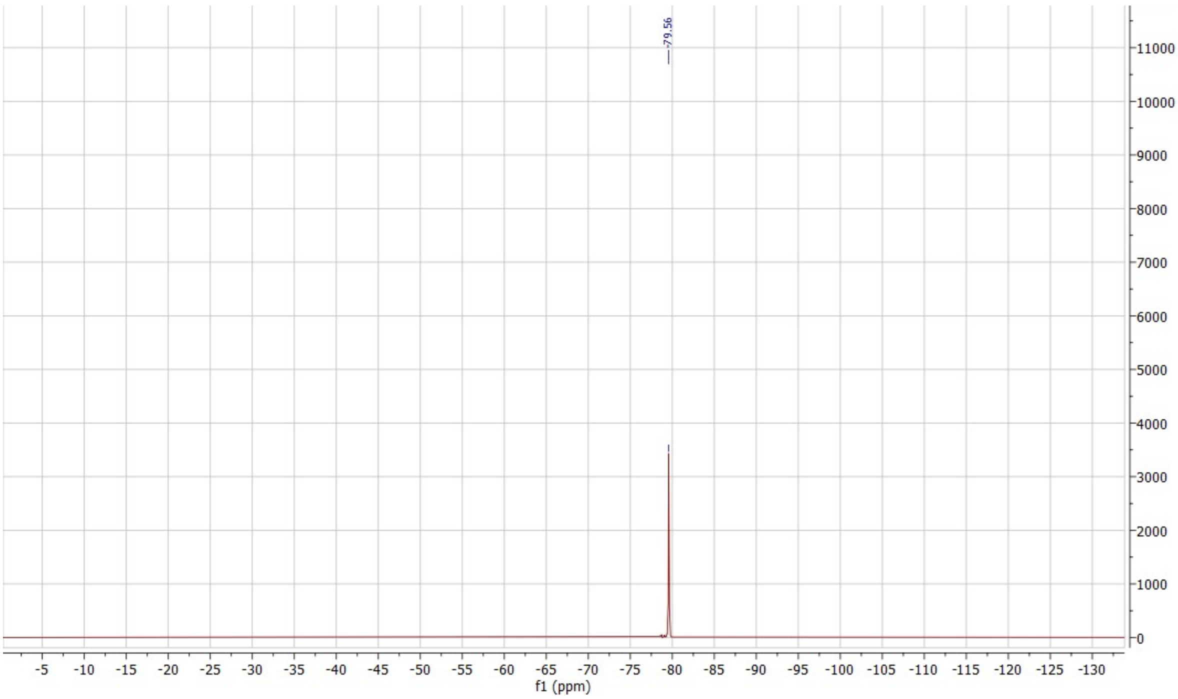

Figure S3. [19]F NMR spectra of Eu(III) coordination polymer **2** in C_6D_6 at 25 °C

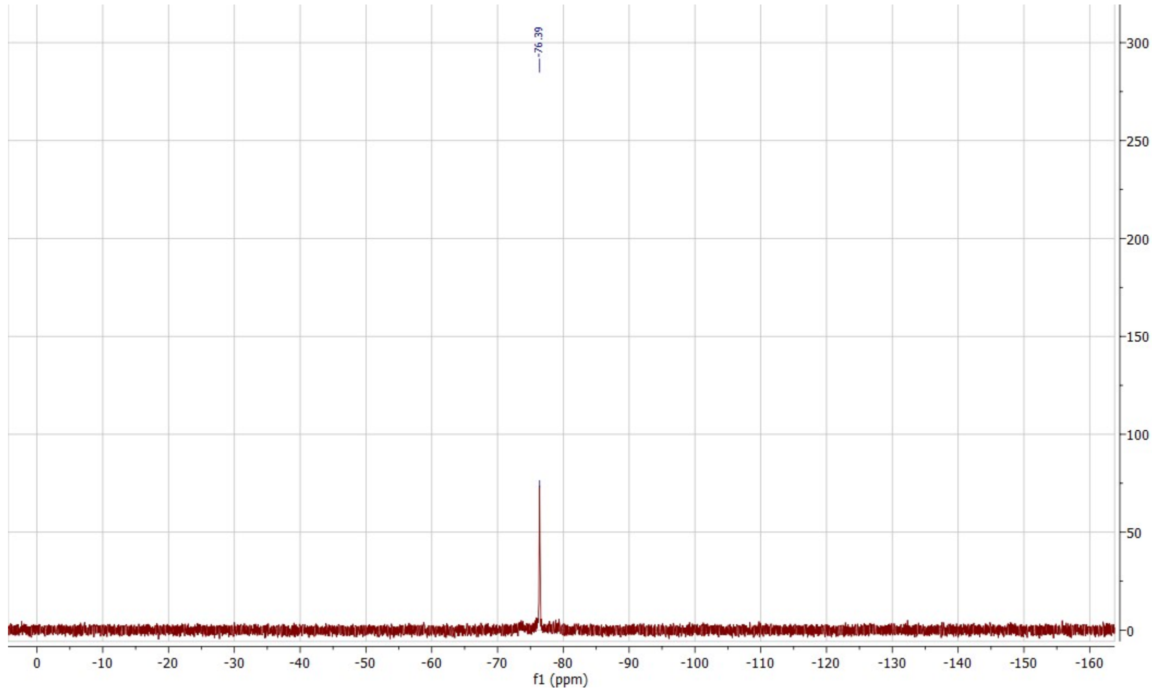

Figure S4. ^{31}P NMR spectra of Eu(III) coordination polymer **2** in C_6D_6 at 25 °C

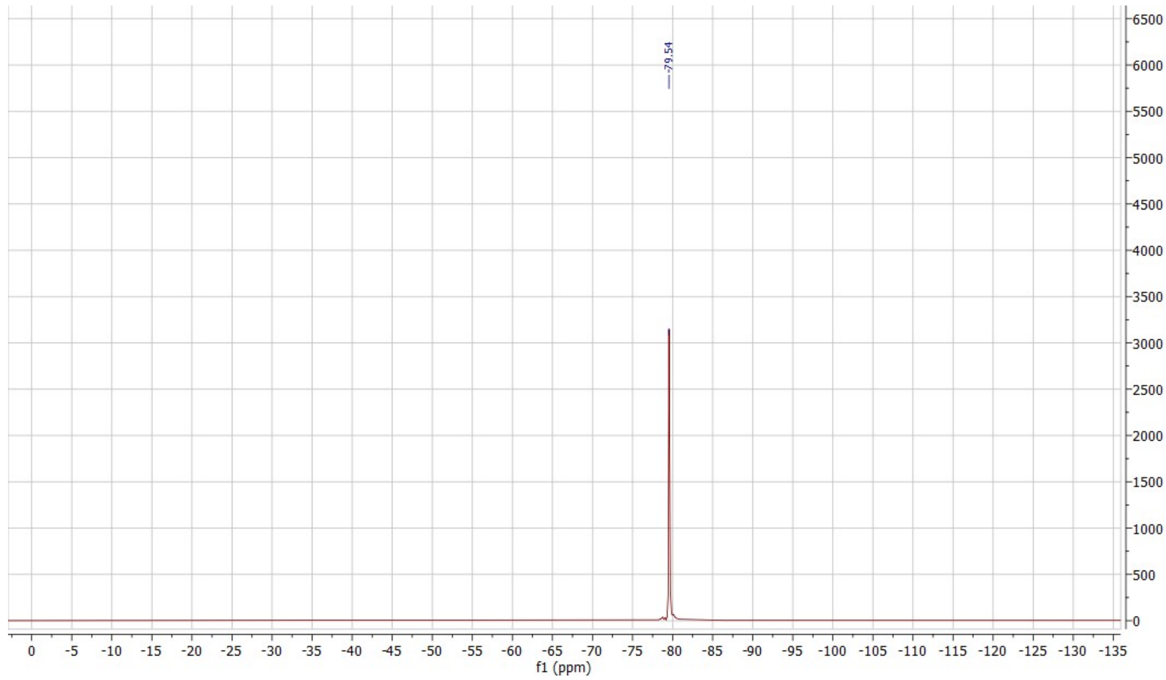

Figure S5. ^{19}F NMR spectra of Eu(III) coordination polymer **3** in C_6D_6 at 25 °C

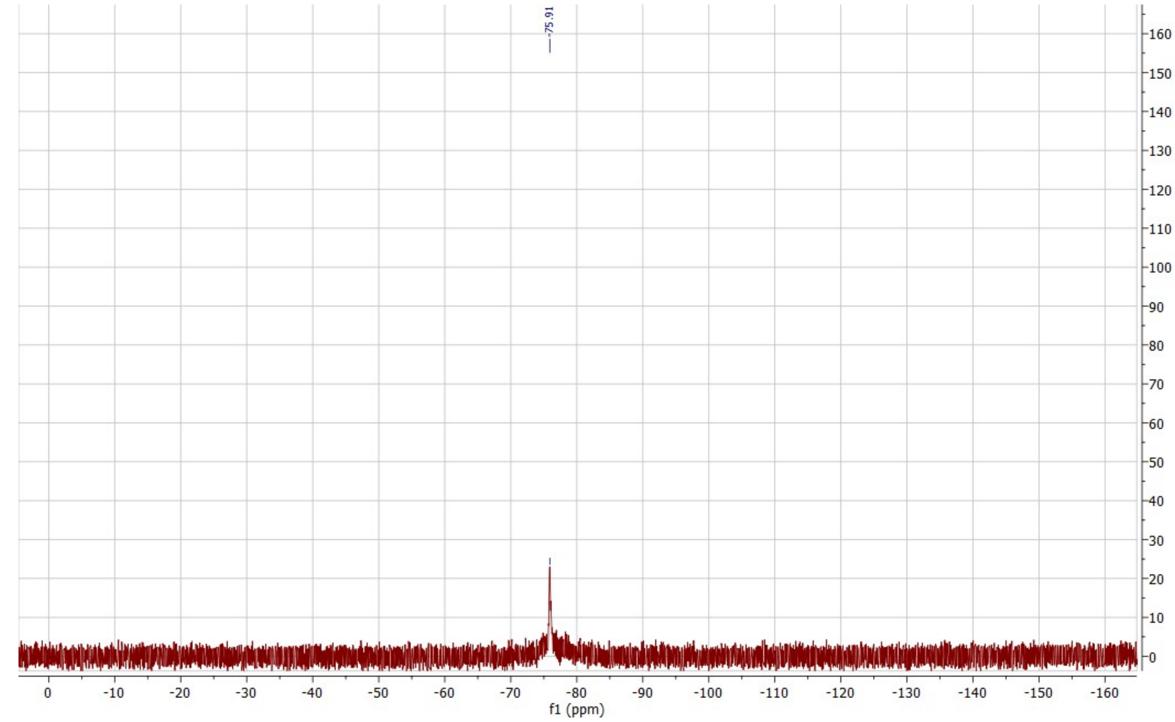

Figure S6. ^{31}P NMR spectra of Eu(III) coordination polymer **3** in C_6D_6 at 25 °C

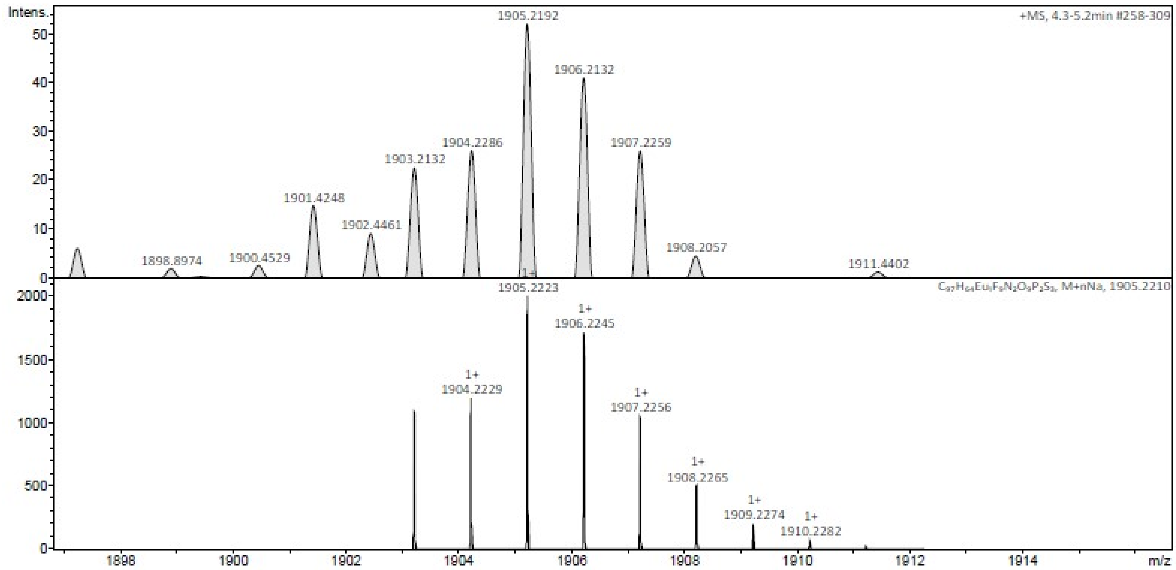

Figure S7. ESI-MS of Eu(III) coordination polymer **1**

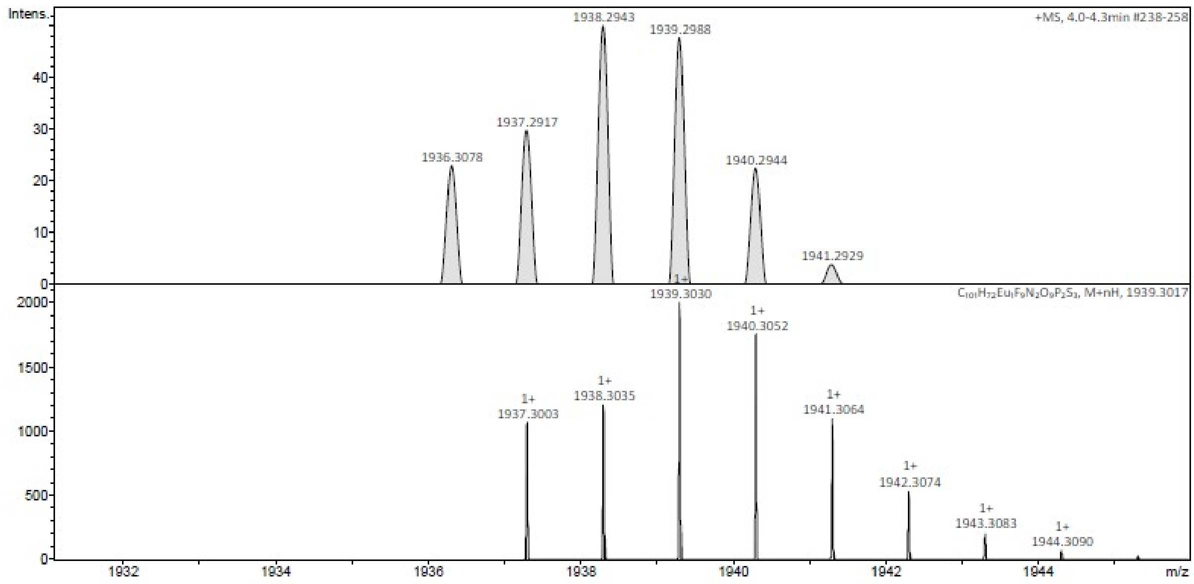

Figure S8. ESI-MS of Eu(III) coordination polymer **2**

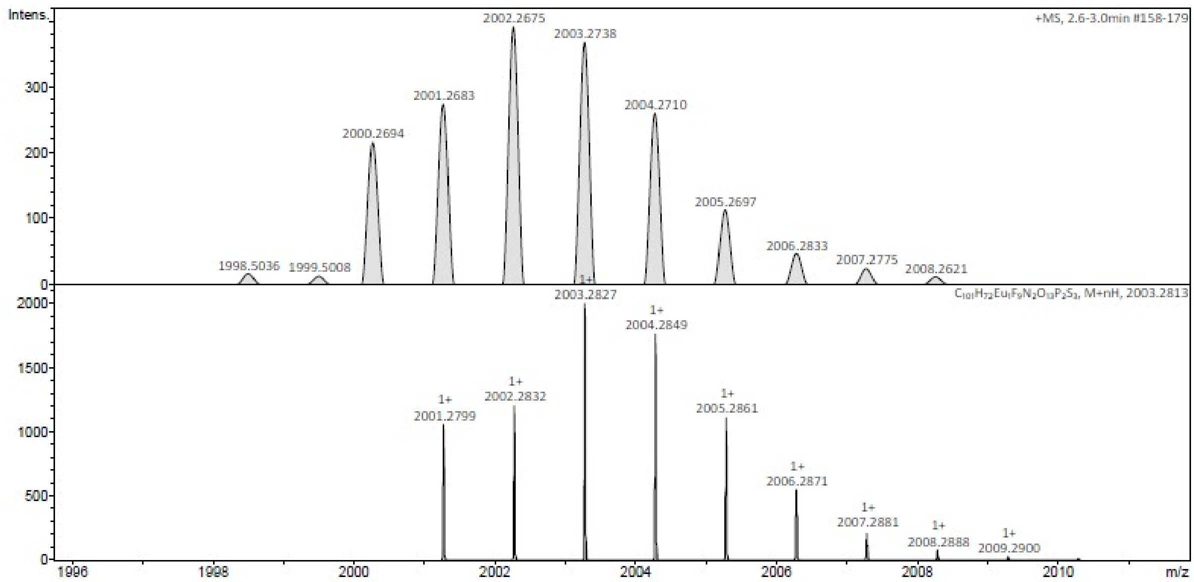

Figure S9. ESI-MS of Eu(III) coordination polymer **3**

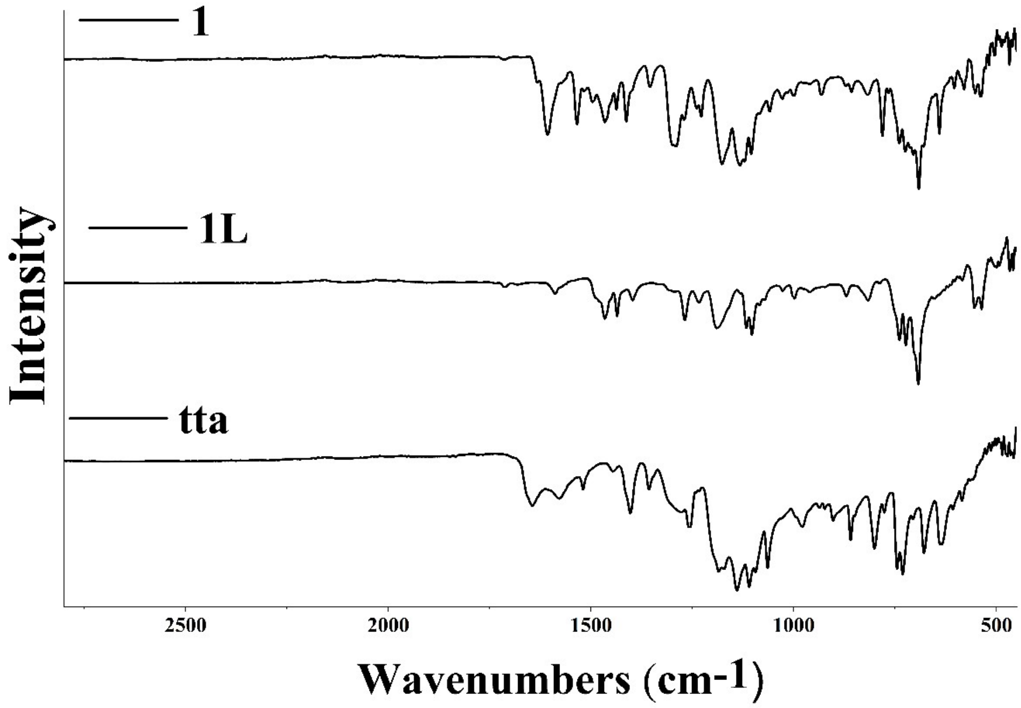

Figure S10. IR spectra of Eu (III) coordination polymer **1** and corresponding ligands

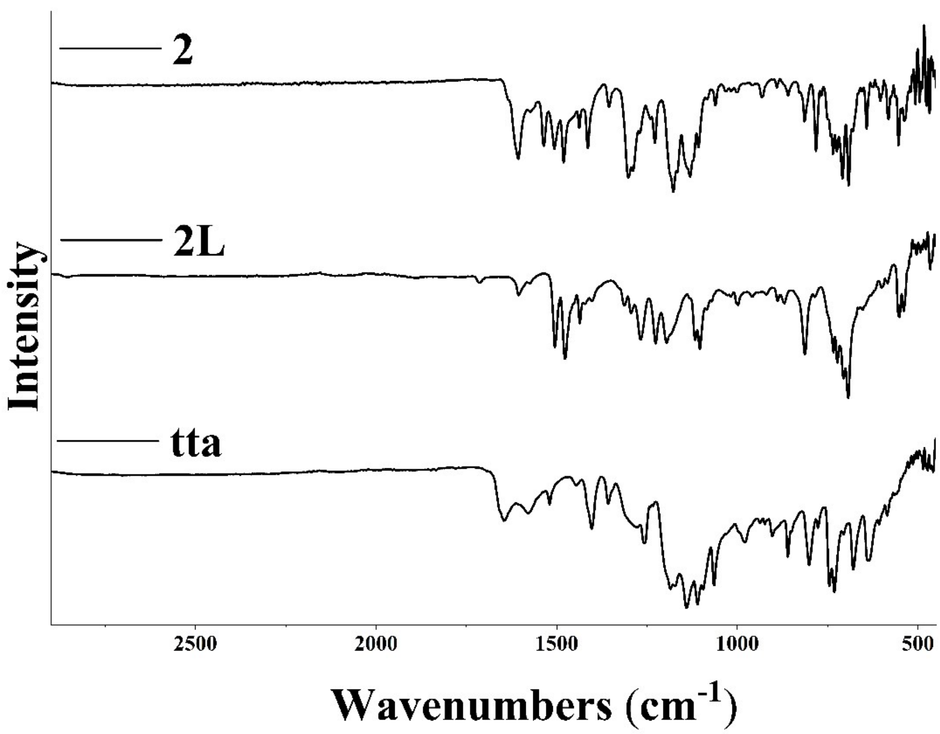

Figure S11. IR spectra of Eu (III) coordination polymer **2** and corresponding ligands

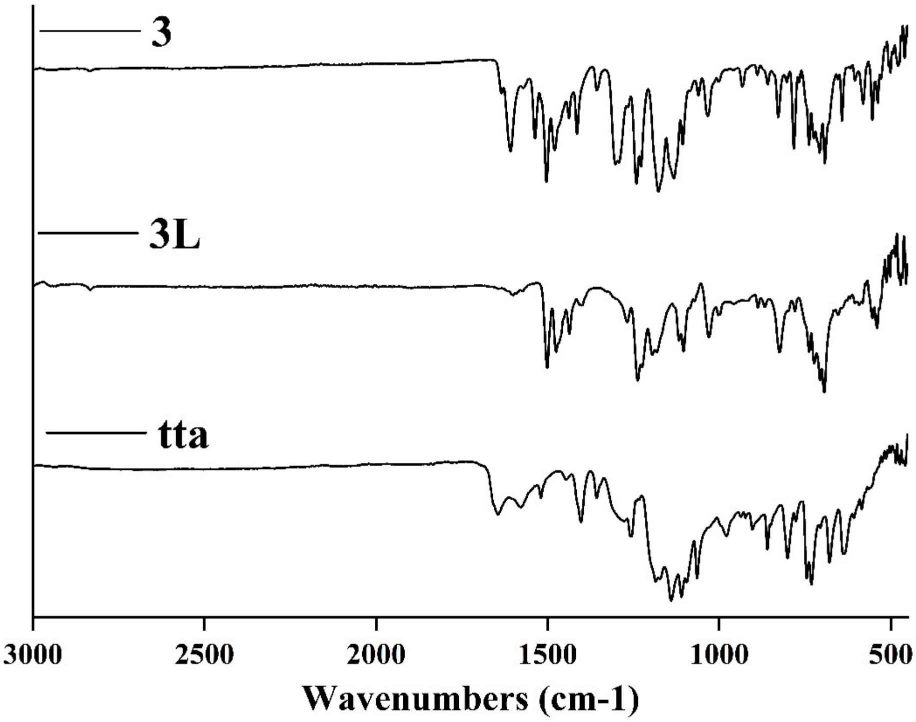

Figure S12. IR spectra of Eu (III) coordination polymer **3** and corresponding ligands

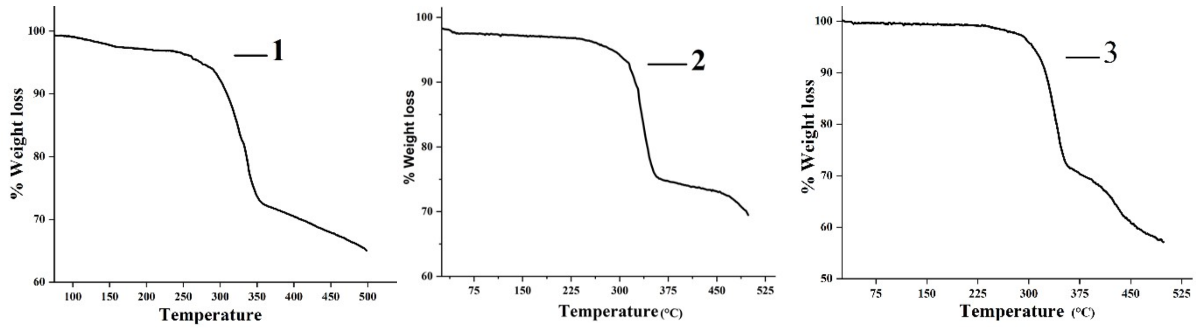

Figure S13. Thermo-Gravimetric Analysis (TGA) of Eu (III) coordination polymer **1**, **2** and **3**

Optical Properties

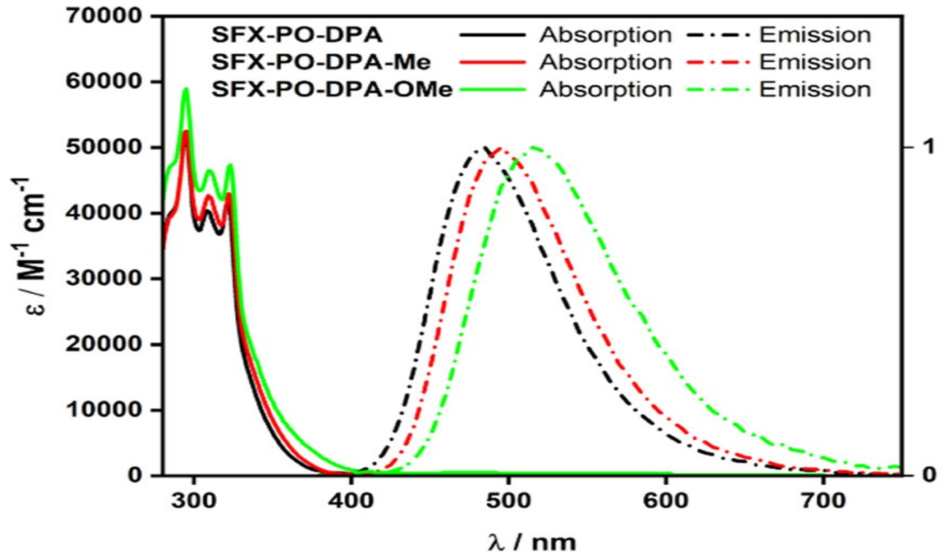

Figure S14. UV-Vis absorption and luminescence spectra of TADF ligands (**SFX-PO-DPA** is **1L**, **SFX-PO-DPA-Me** is **2L** and **SFX-PO-DPA-OMe** is **3L**) in toluene solution (Adapted from ref 1, Copyright, 2021, American Chemical Society).[1]

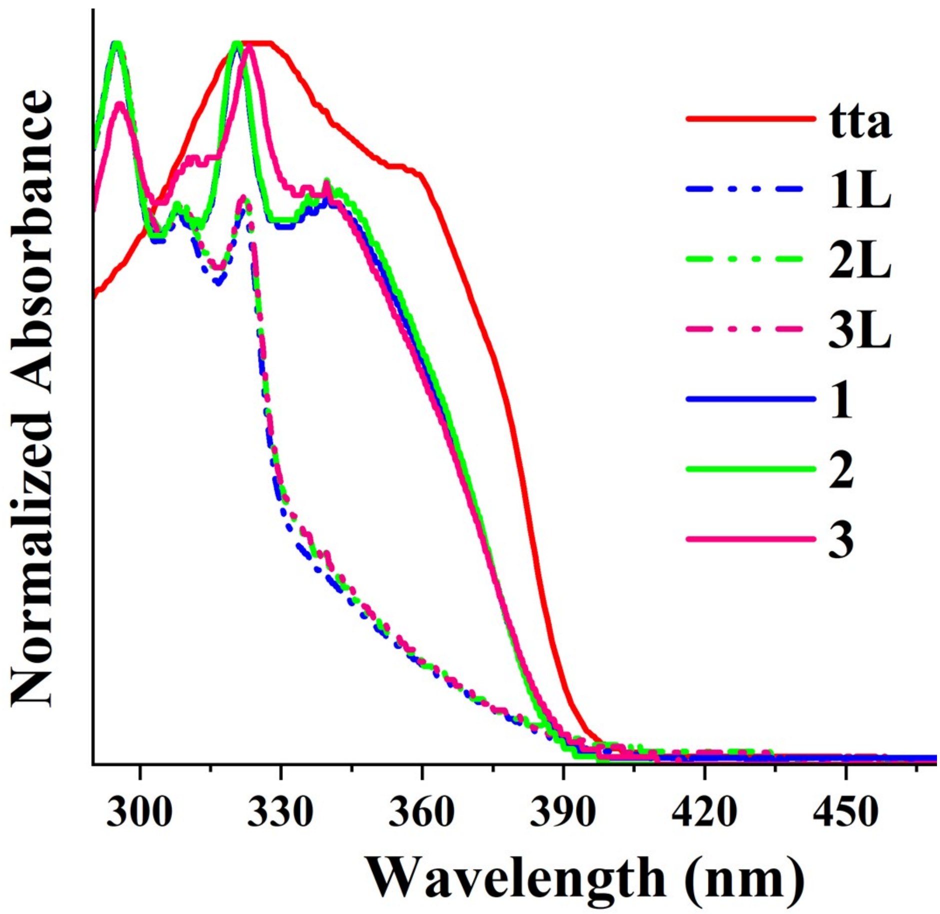

Figure S15. Comparison of UV-Vis absorption spectra of tta, TADF ligands (**1L**, **2L**, and **3L**) and corresponding Eu(III) coordination polymers (**1**, **2** and **3**) in toluene solution

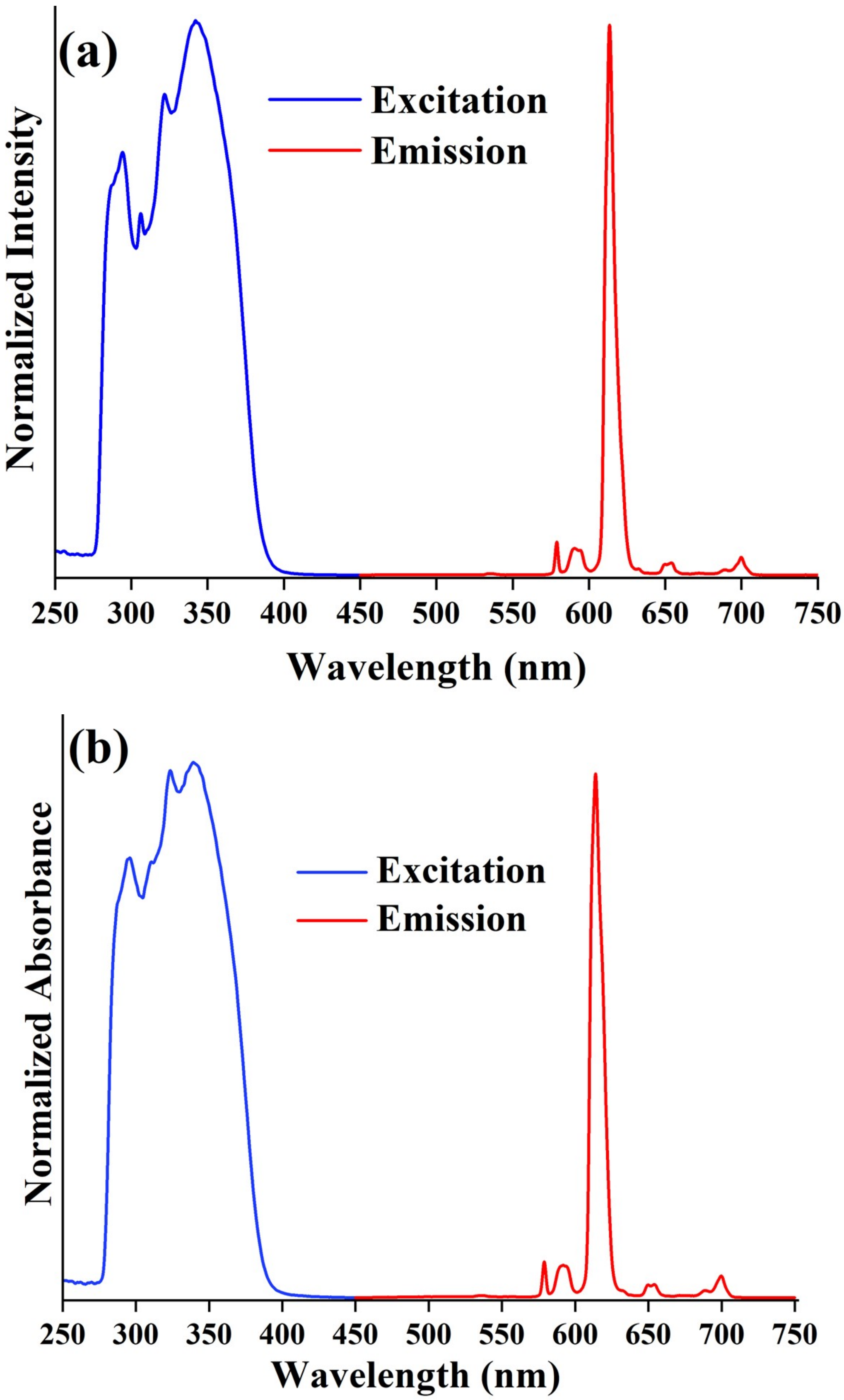

Figure S16. Excitation and luminescence spectra of (a) **1** (b) **2** in toluene solution (λ_{ex}= 340 nm and λ_{em}= 611 nm)

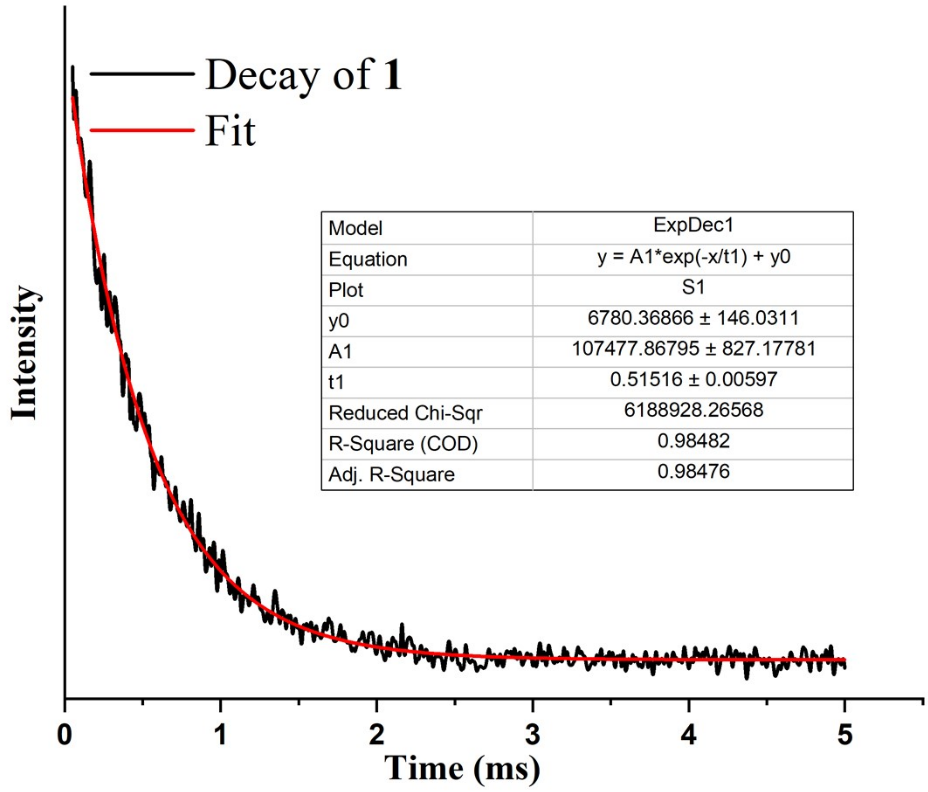

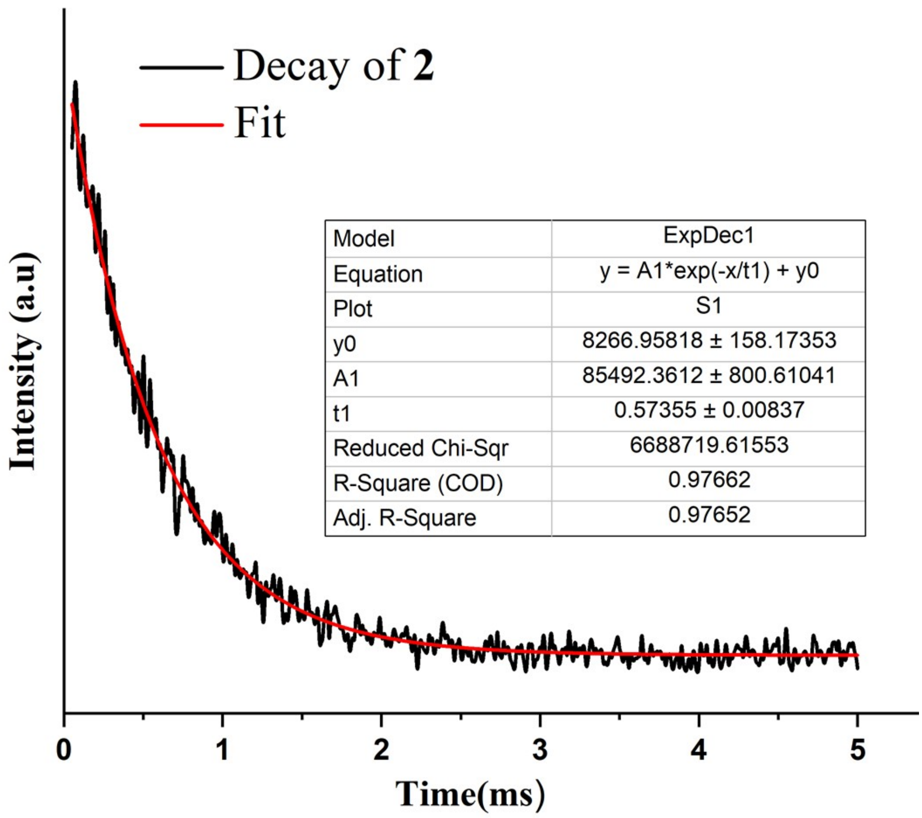

Figure S17. Luminescence decay profiles of complexes **1** and **2** in toluene solution (λ_{ex}=340 and λ_{em}=611 nm)

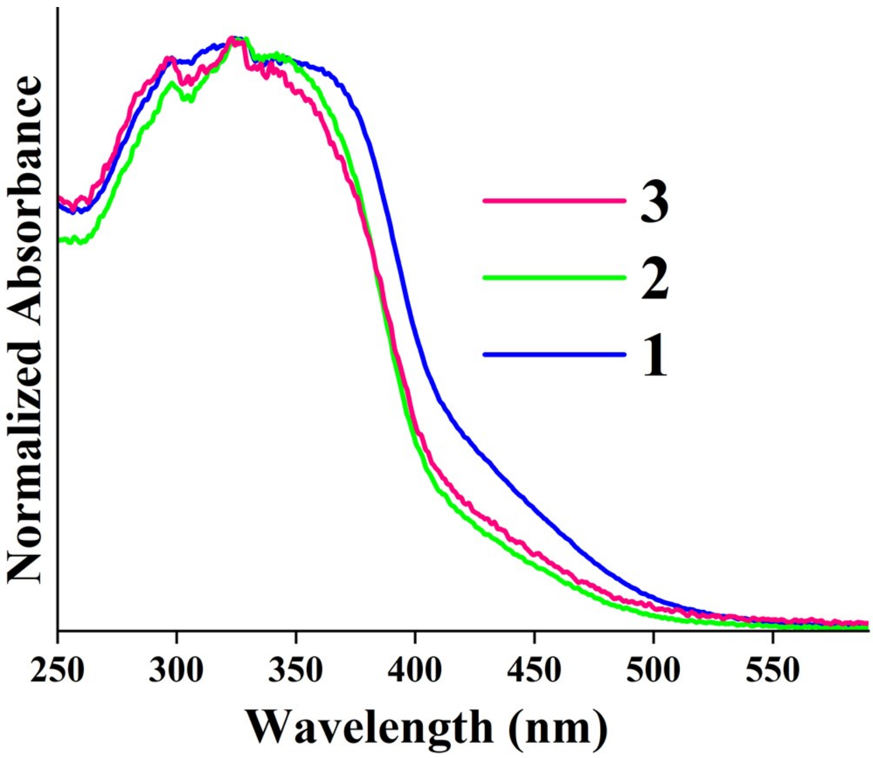

Figure S18. UV-Vis absorption spectra of powder samples of **1**-**3**

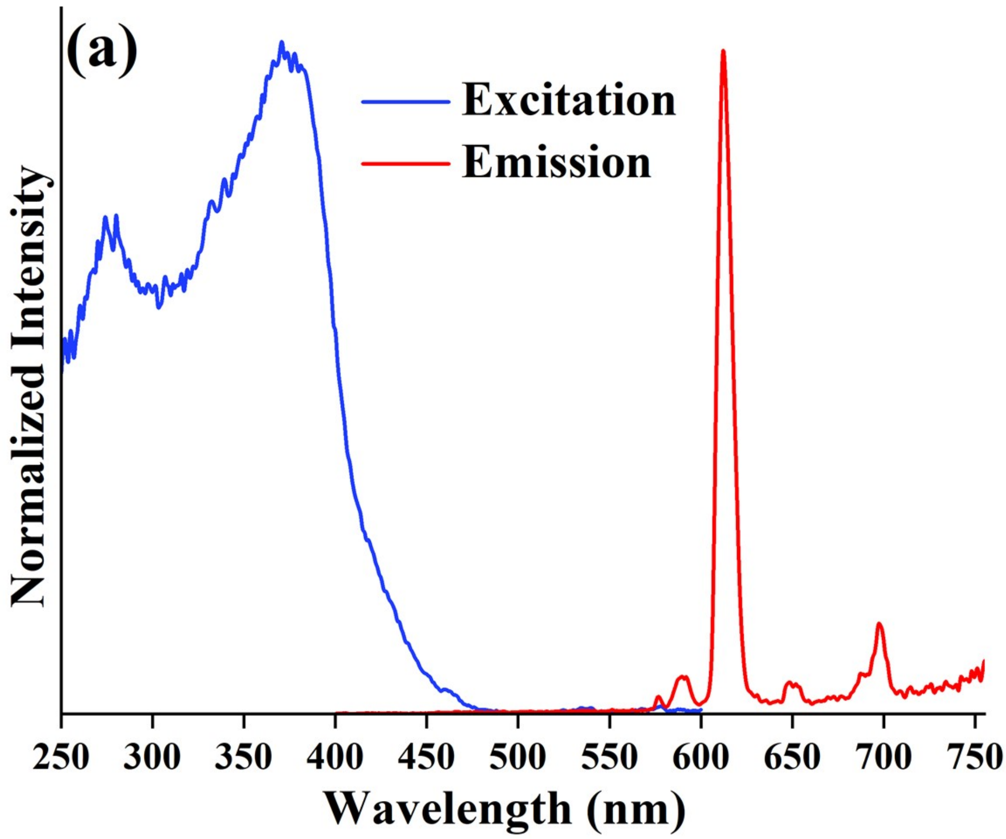

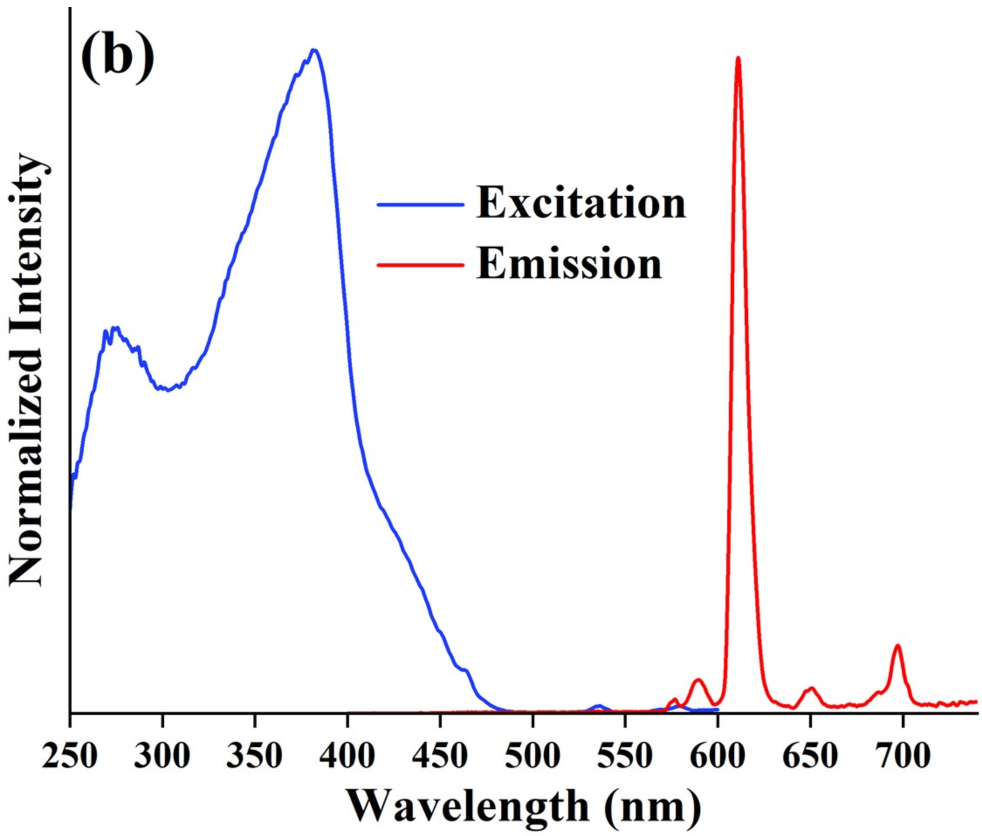

Figure S19. Excitation and luminescence spectra of (a) **1** (b) **2** powder samples (λ_{ex}= 340 nm and λ_{em}= 611 nm)

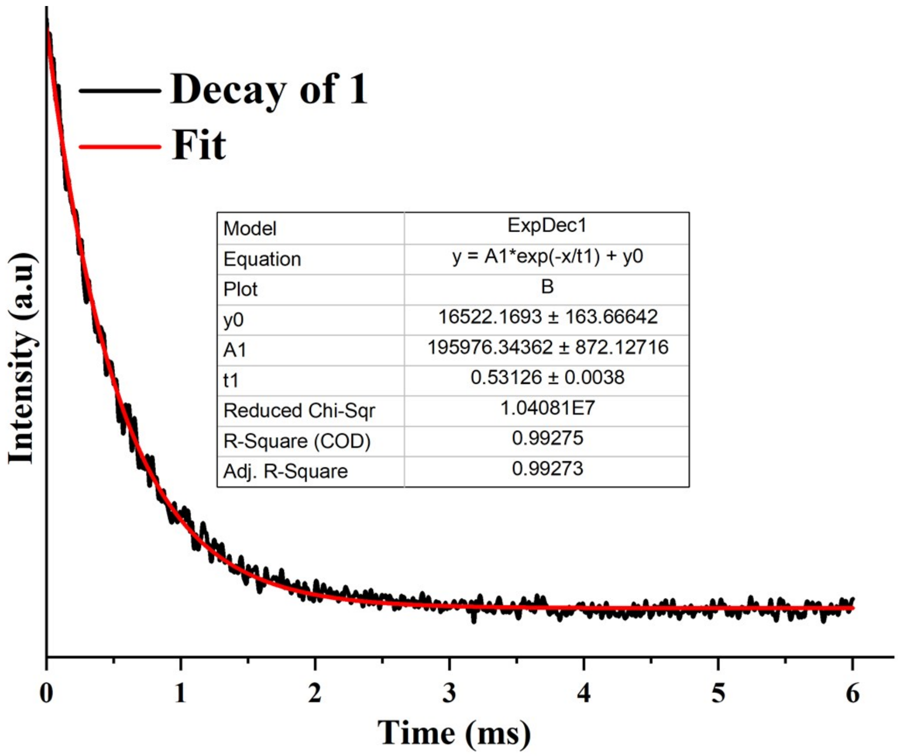

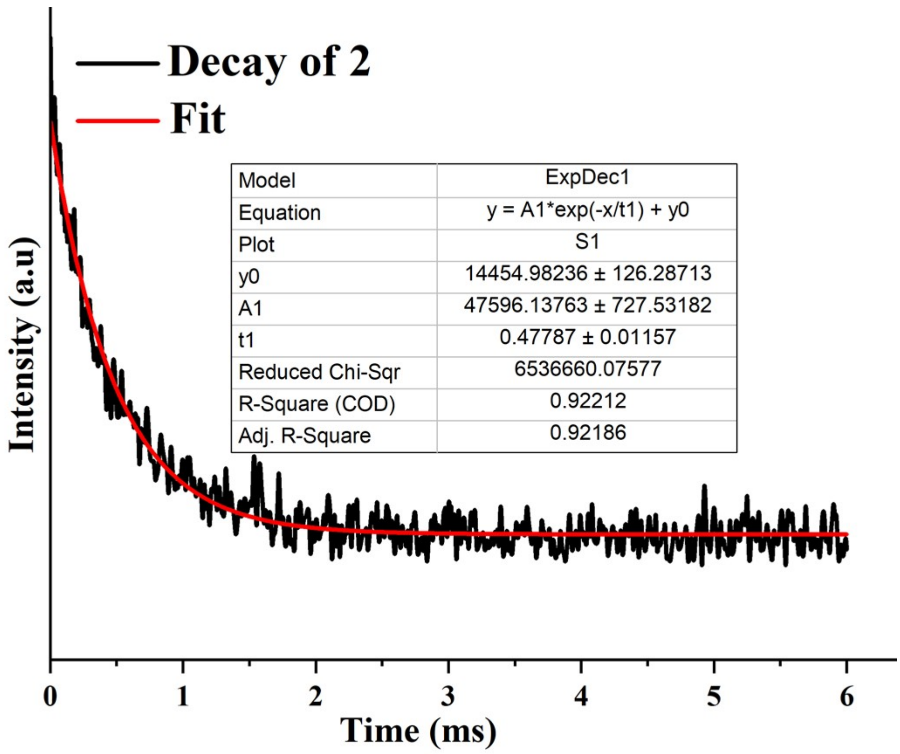

Figure S20. Luminescence decay profiles of powder samples of complexes **1** and **2** (λ_{ex}=340 and λ_{em}=611 nm)

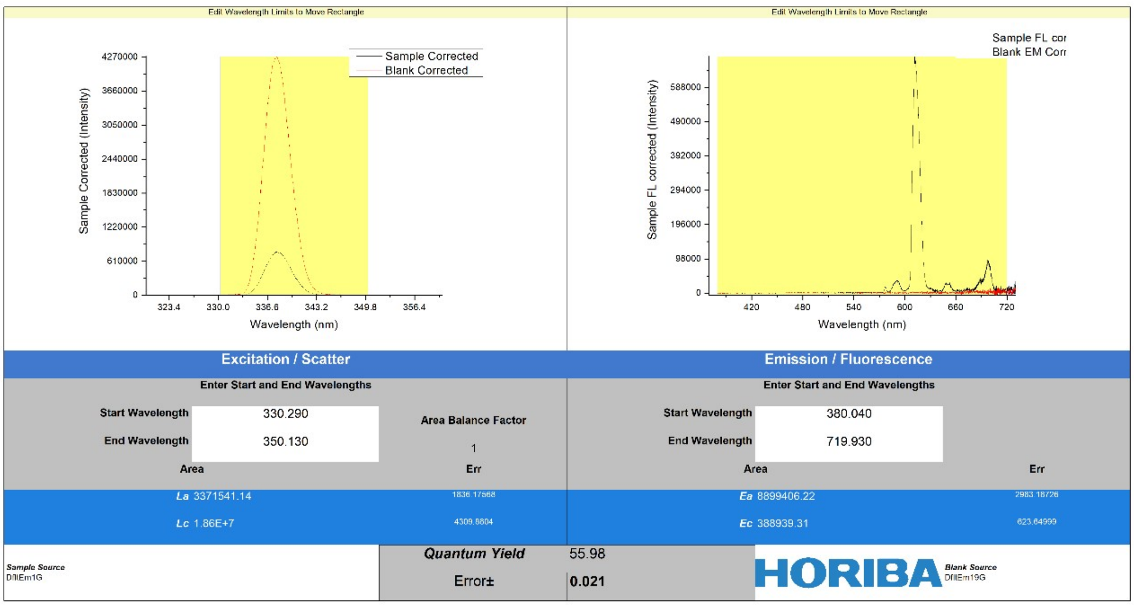

Figure S21. Absolute luminescence quantum yield measurements of solid samples of **1** (λ_{ex}=340)

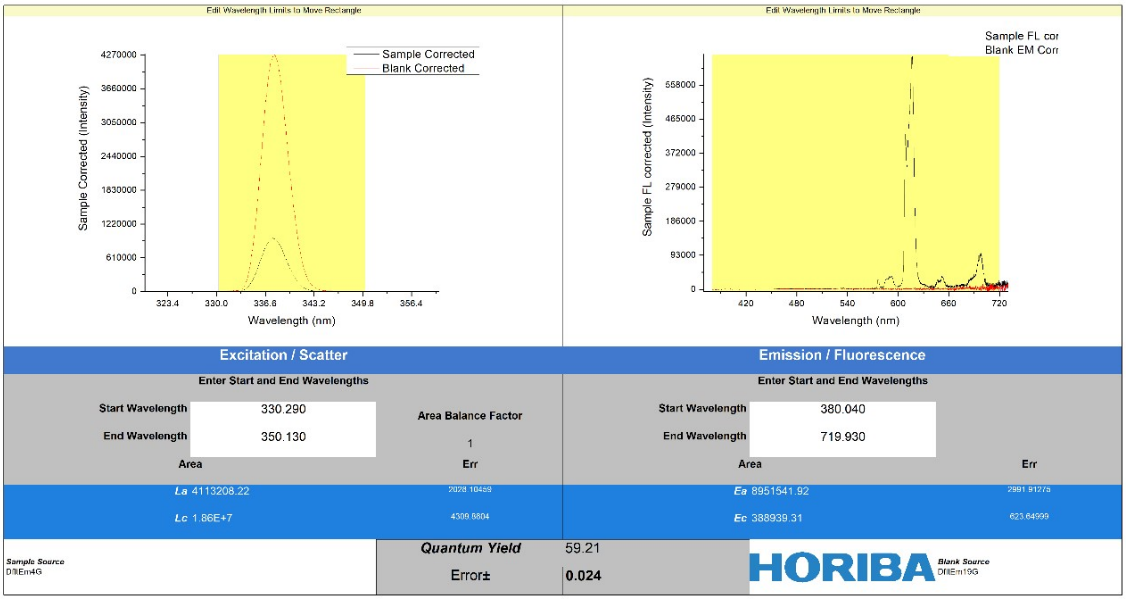

Figure S22. Absolute luminescence quantum yield measurements of solid samples of **2** (λ_{ex}=340)

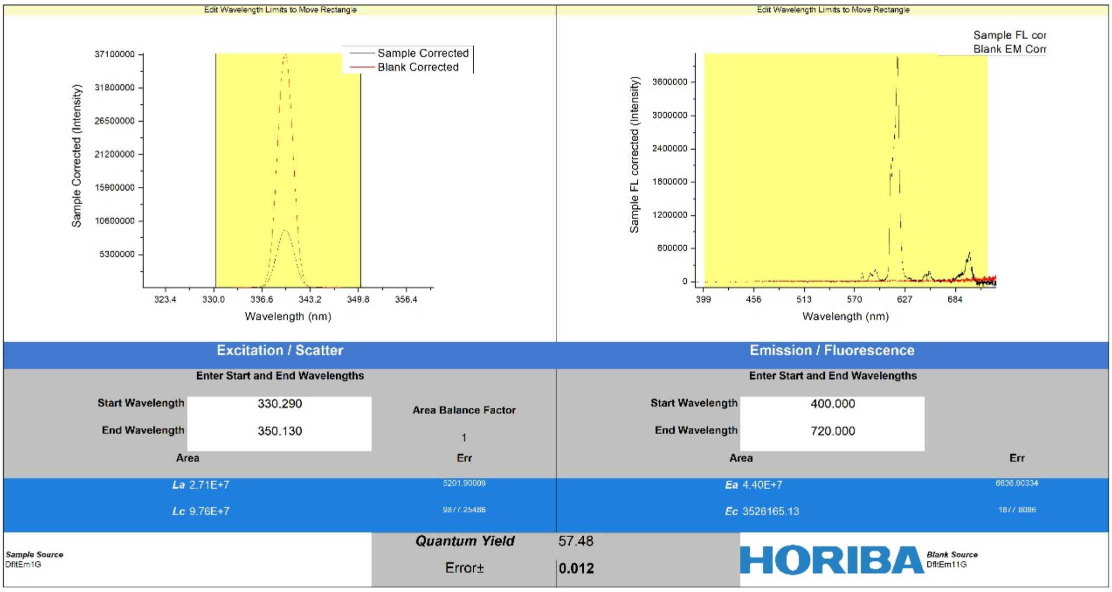

Figure S23. Absolute luminescence quantum yield measurements of solid samples of **3** (λ_{ex}=340)

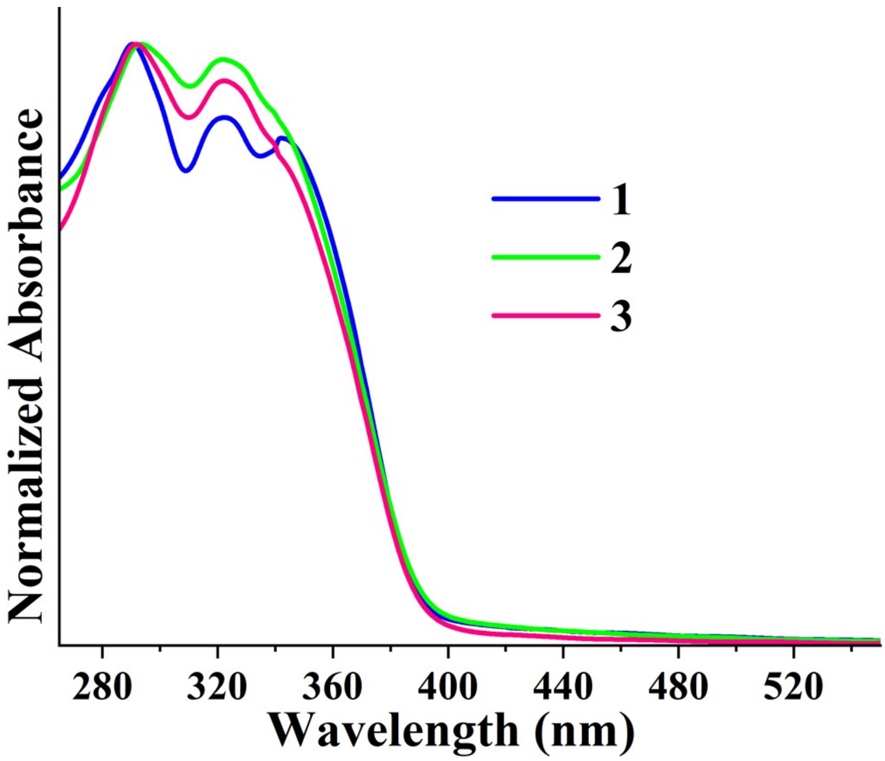

Figure S24. UV-Vis absorption spectra of PMMA encapsulated films of **1**-**3**

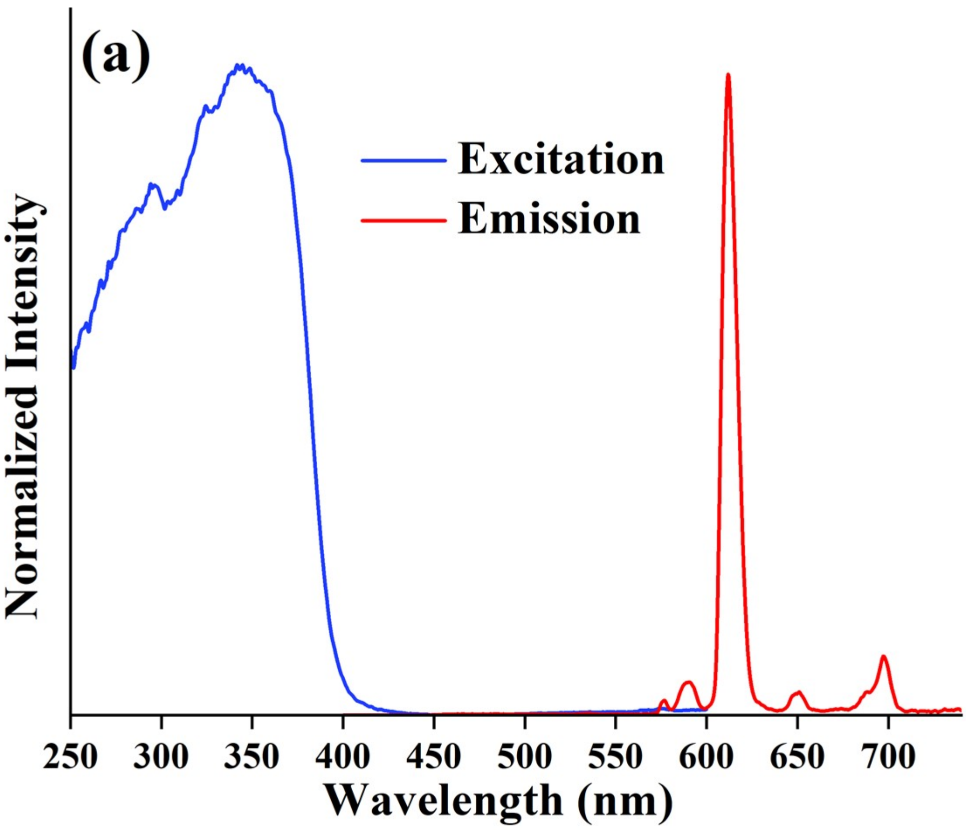

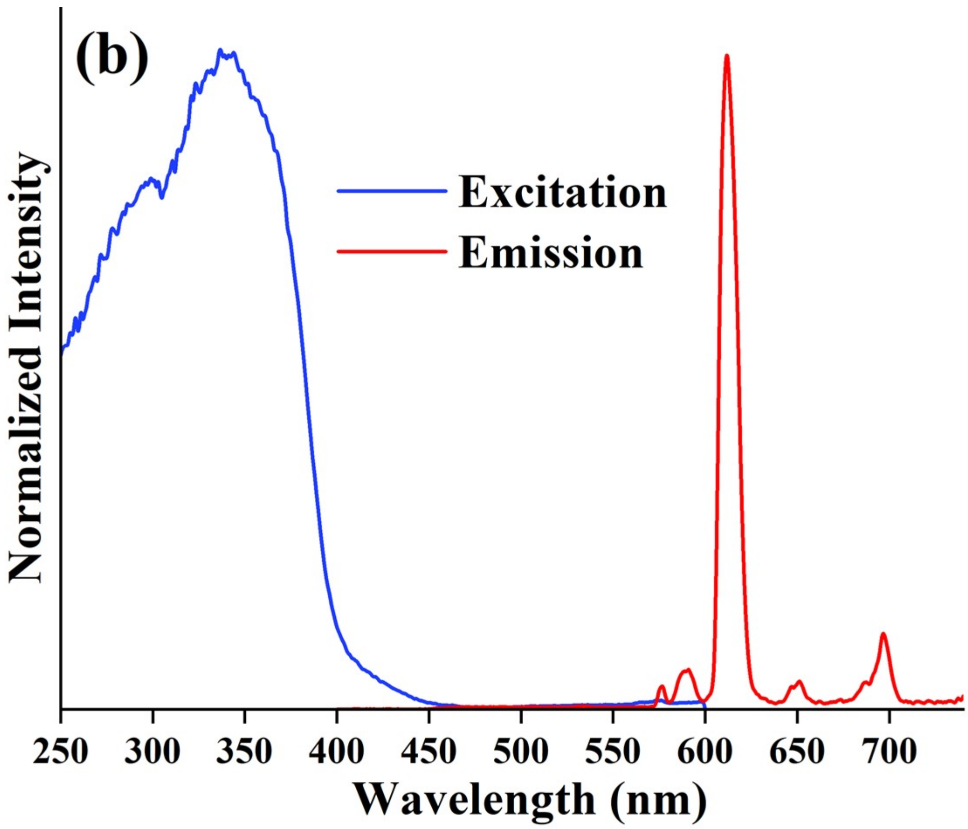

Figure S25. Excitation and luminescence spectra of PMMA encapsulated films (a) **1** and (b) **3** (λ_{ex}= 340 nm and λ_{em}= 611 nm)

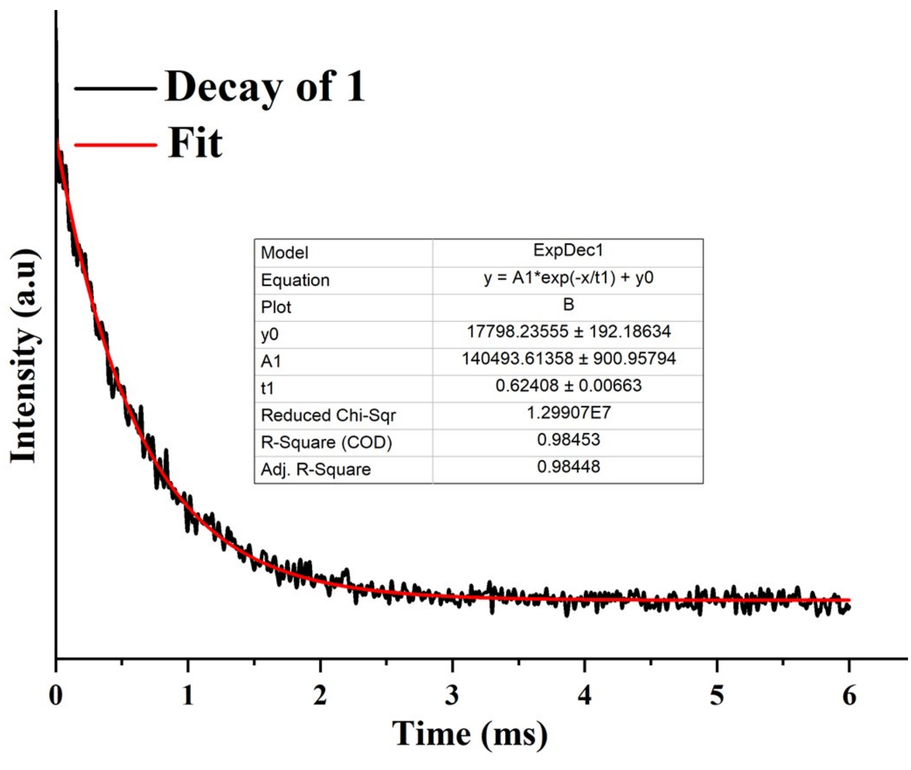

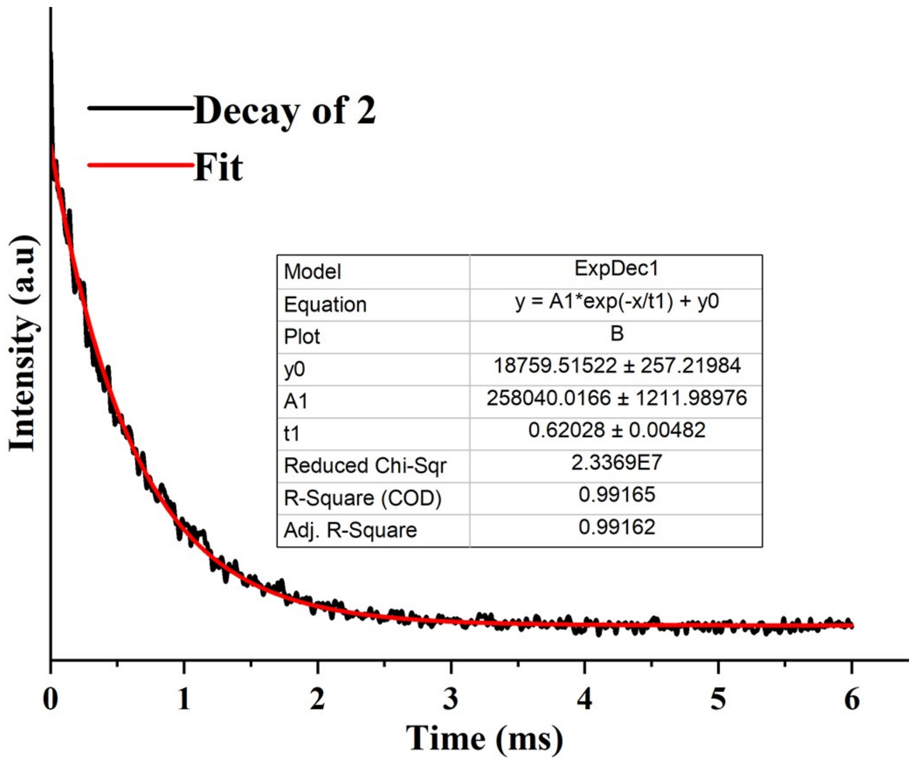

Figure S26. Luminescence decay profiles of complexes **1** and **2** in PMMA films (λ_{ex}=340 and λ_{em}=611 nm)

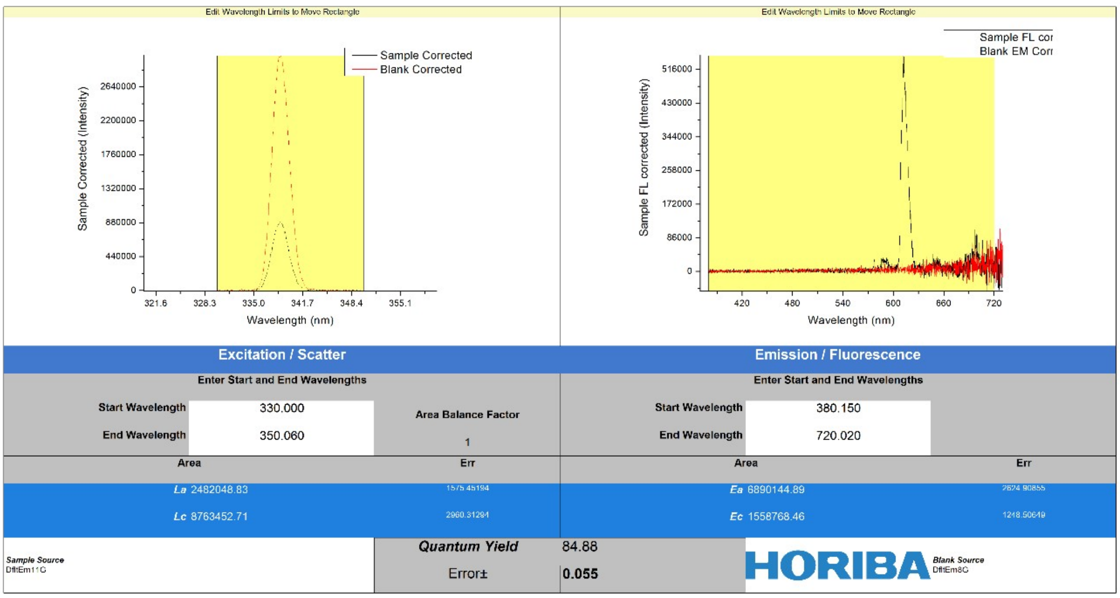

Figure S27. Absolute luminescence quantum yield measurements of PMMA encapsulated films of **1** (λ_{ex}=340)

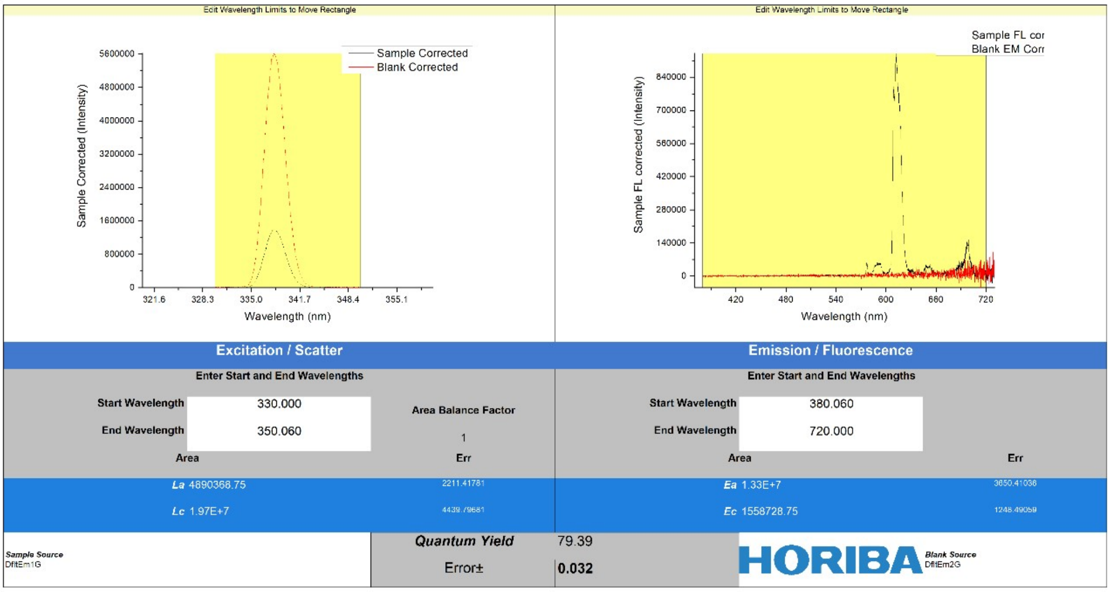

Figure S28. Absolute luminescence quantum yield measurements of PMMA encapsulated films of **2** (λ_{ex}=340)

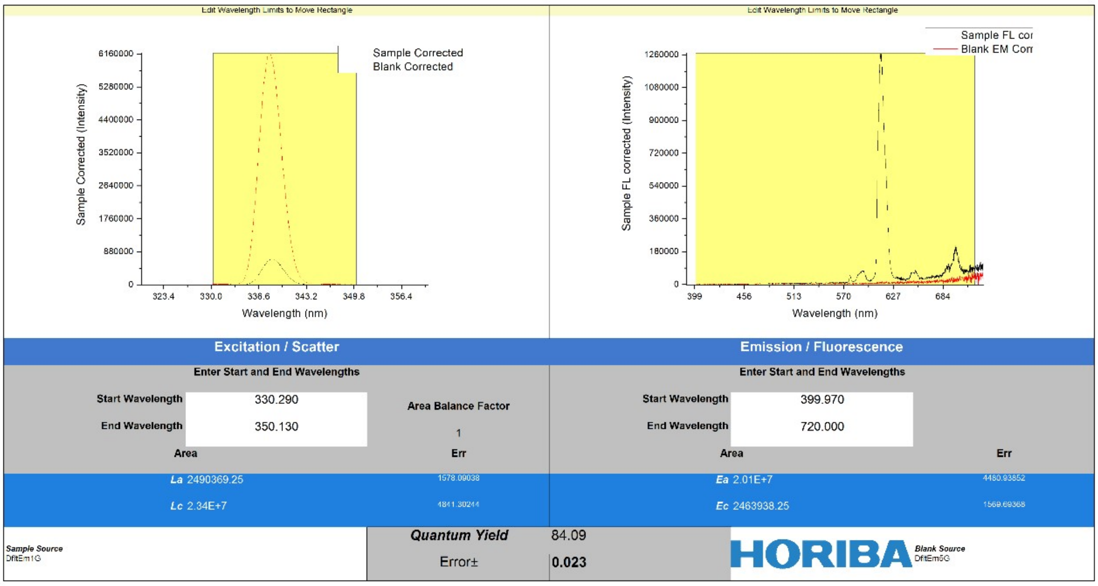

Figure S29. Absolute luminescence quantum yield measurements of PMMA encapsulated films of **3** (λ_{ex}=340)

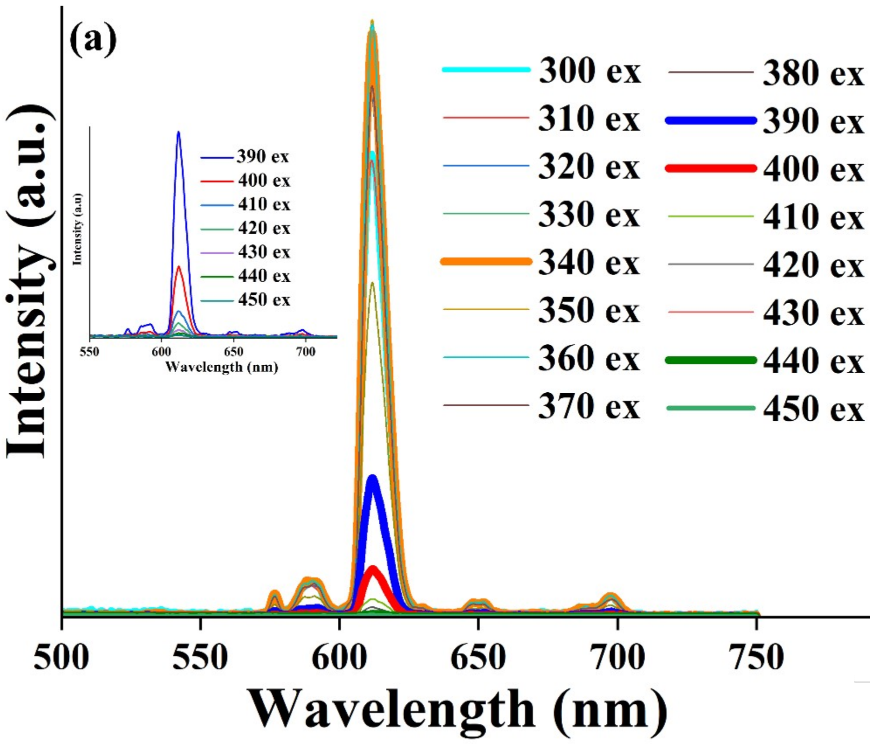

Figure S30. Luminescence spectra of PMMA encapsulated films of **1** at different excitations in the region 300-450 nm

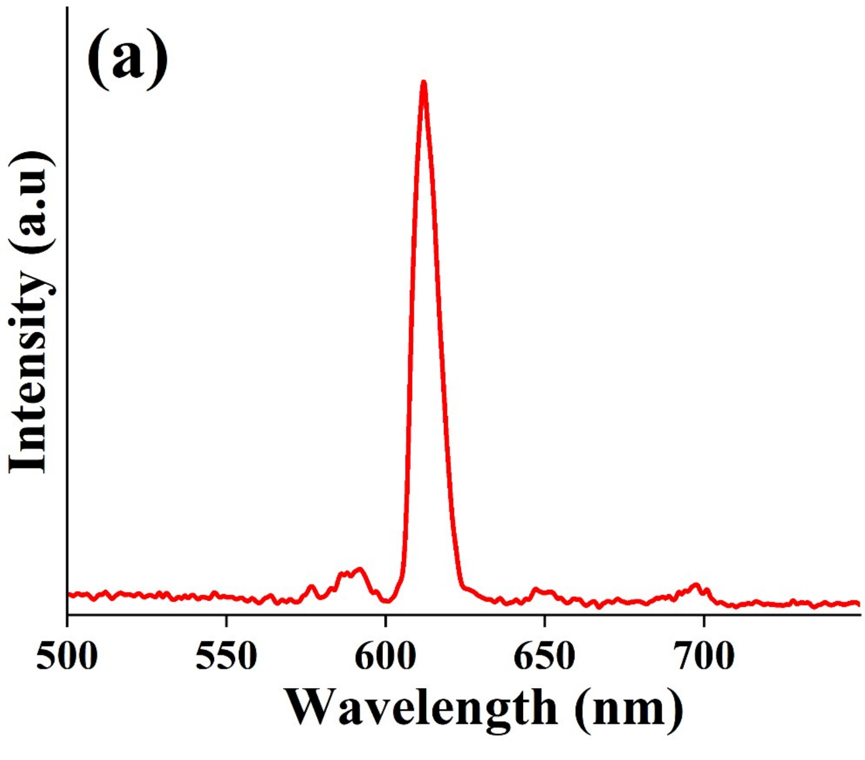

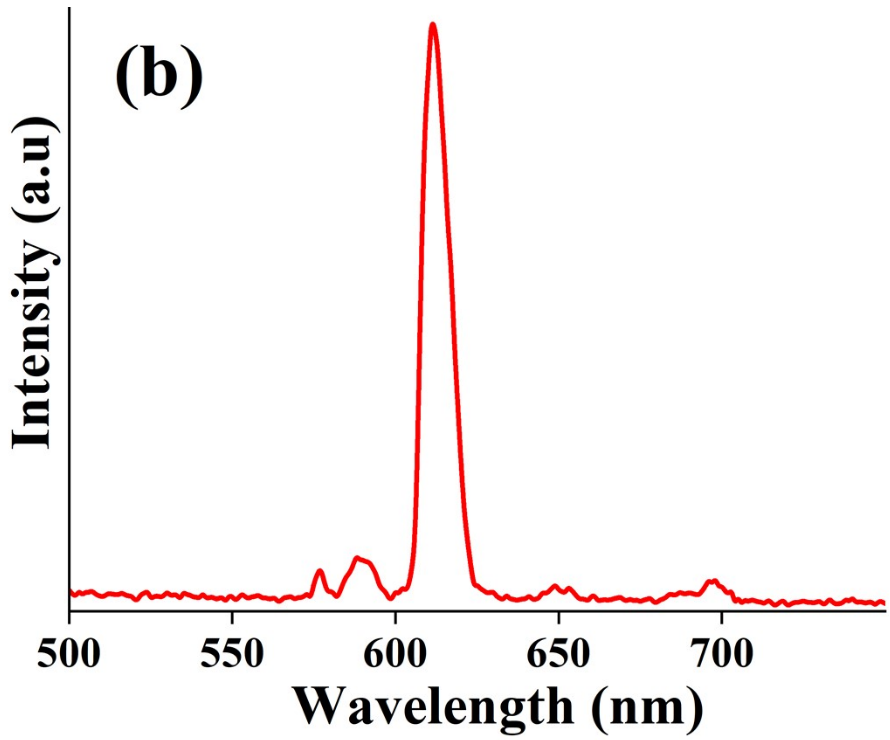

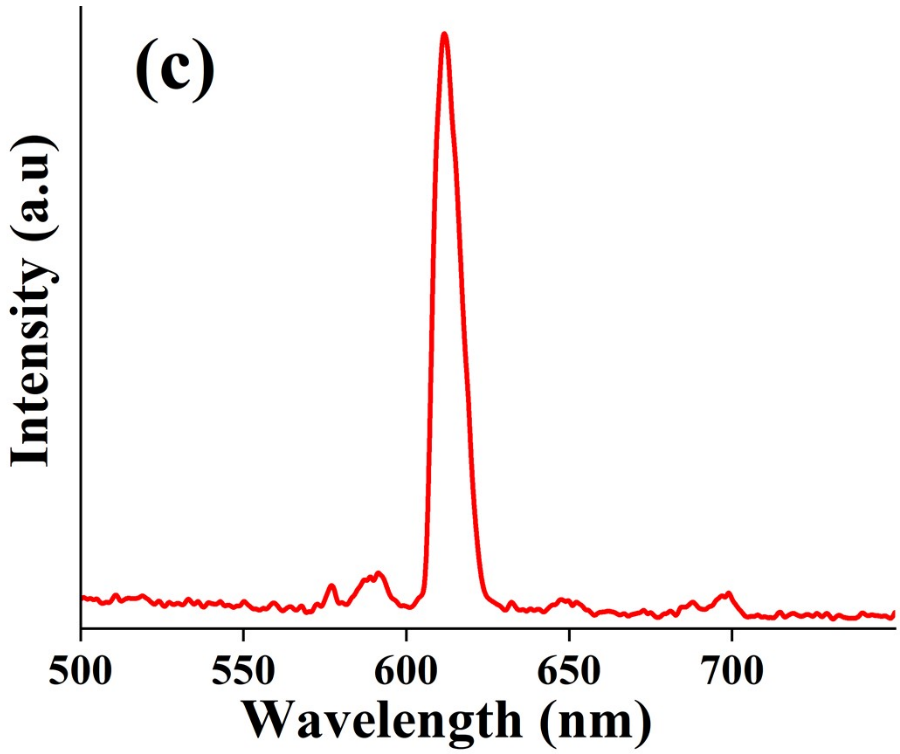

Figure S31. Luminescence spectra of PMMA encapsulated films (a) **1** (b) **2** and (c) **3** (λ_{ex}= 400 nm)

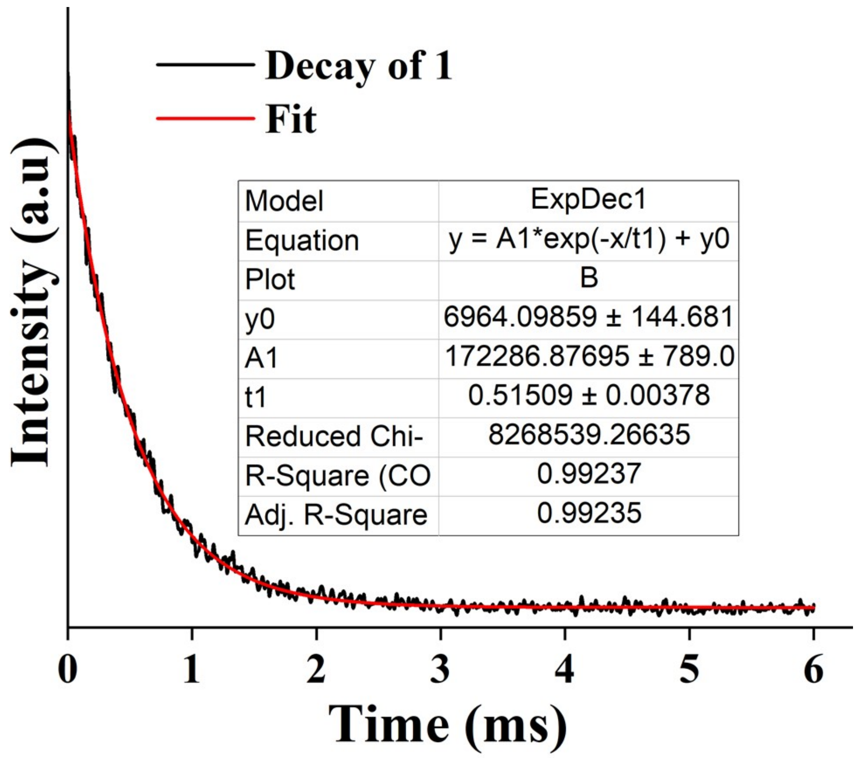
Decay of 1
Fit
Model | ExpDec1
Equation | y = A1*exp(-x/t1) + y0
Plot | B
y0 | 6964.09859 ± 144.681
A1 | 172286.87695 ± 789.0
t1 | 0.51509 ± 0.00378
Reduced Chi- | 8268539.26635
R-Square (CO | 0.99237
Adj. R-Square | 0.99235
Intensity (a.u)
0
1
2
3
4
5
6
Time (ms)

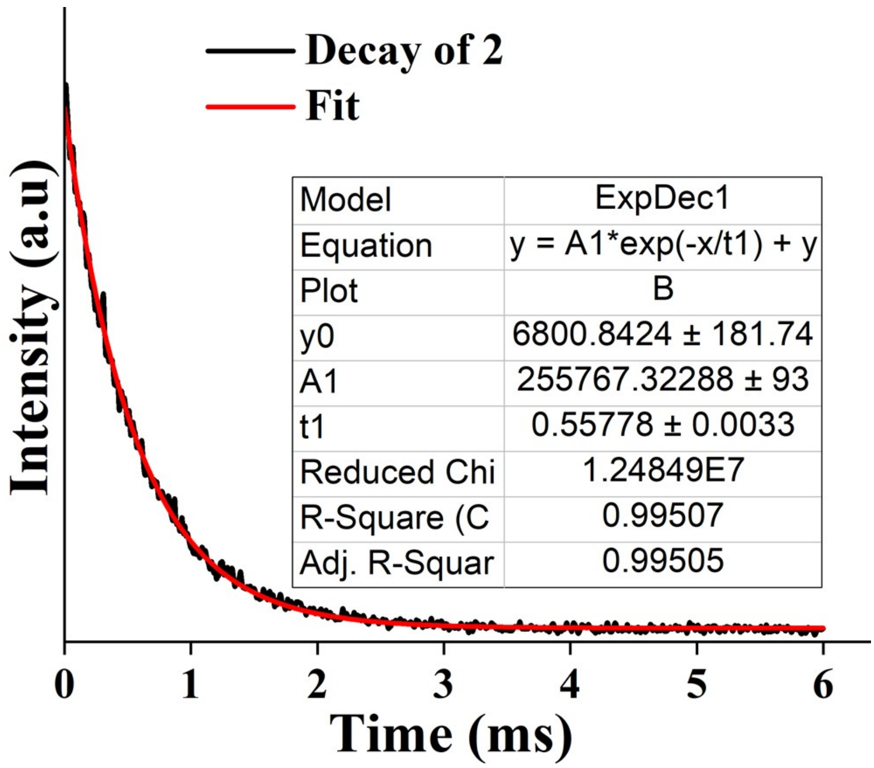
Decay of 2
Fit
Model | ExpDec1
Equation | y = A1*exp(-x/t1) + y
Plot | B
y0 | 6800.8424 ± 181.74
A1 | 255767.32288 ± 93
t1 | 0.55778 ± 0.0033
Reduced Chi | 1.24849E7
R-Square (C | 0.99507
Adj. R-Squar | 0.99505
Intensity (a.u)
0
1
2
3
4
5
6
Time (ms)

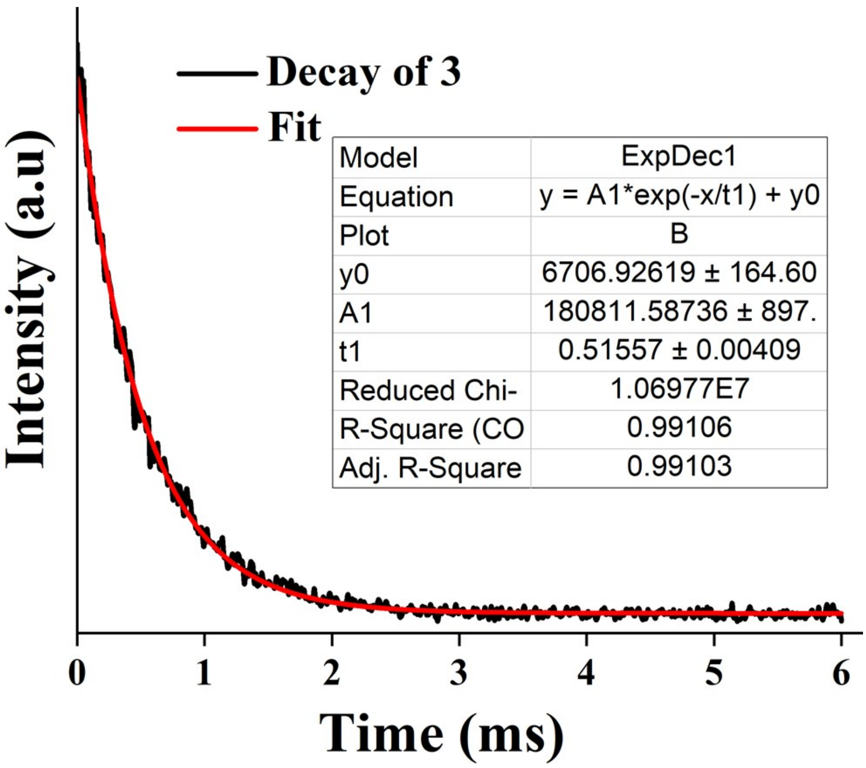

Figure S32. Luminescence decay profiles of **1**-**3** in PMMA encapsulated films (λ_{ex}=400 and λ_{em}=611 nm)

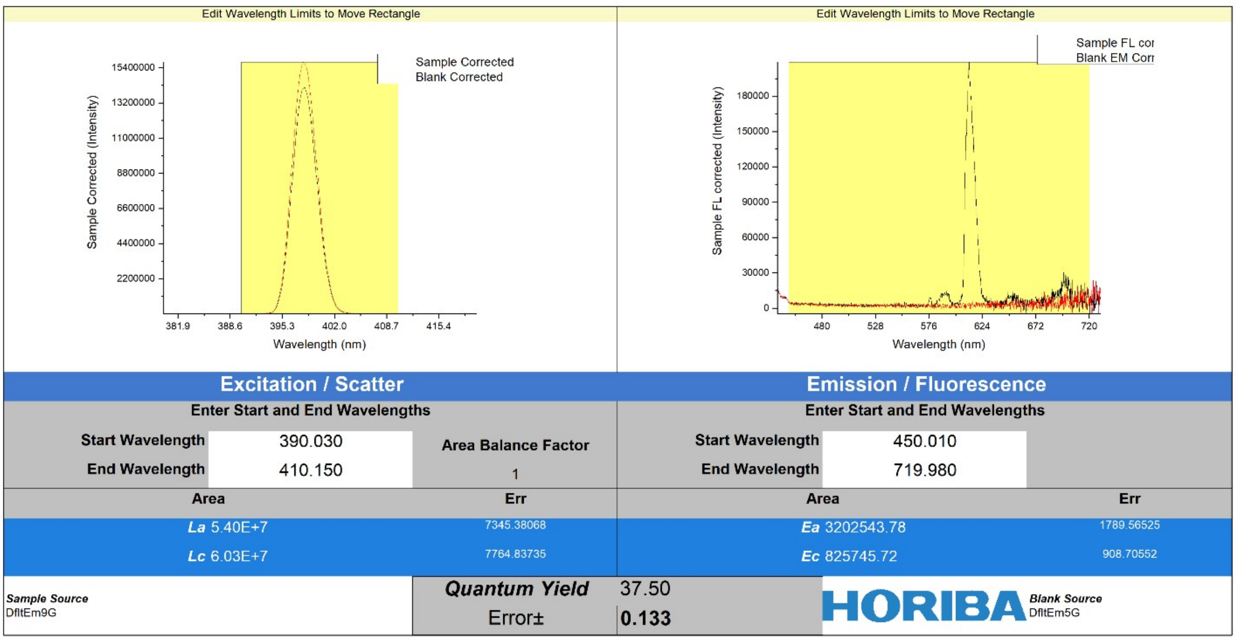

Figure S33. Absolute luminescence quantum yield measurements of PMMA encapsulated films of **1** (λ_{ex}=400)

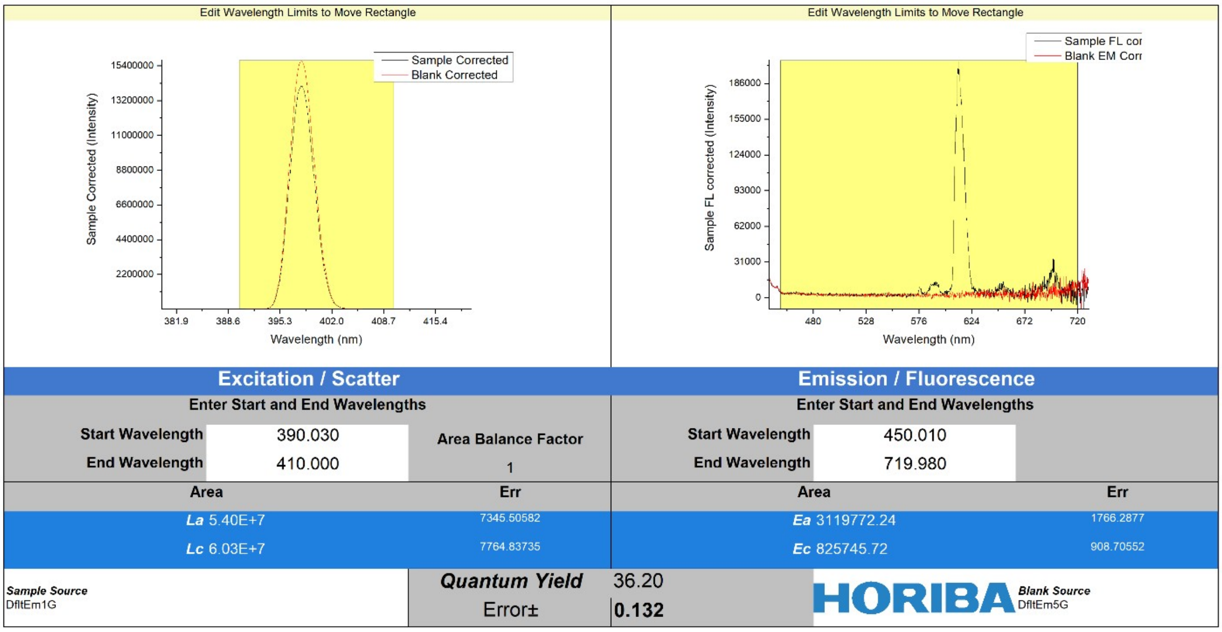

Figure S34. Absolute luminescence quantum yield measurements of PMMA encapsulated films of **2** (λ_{ex}=400)

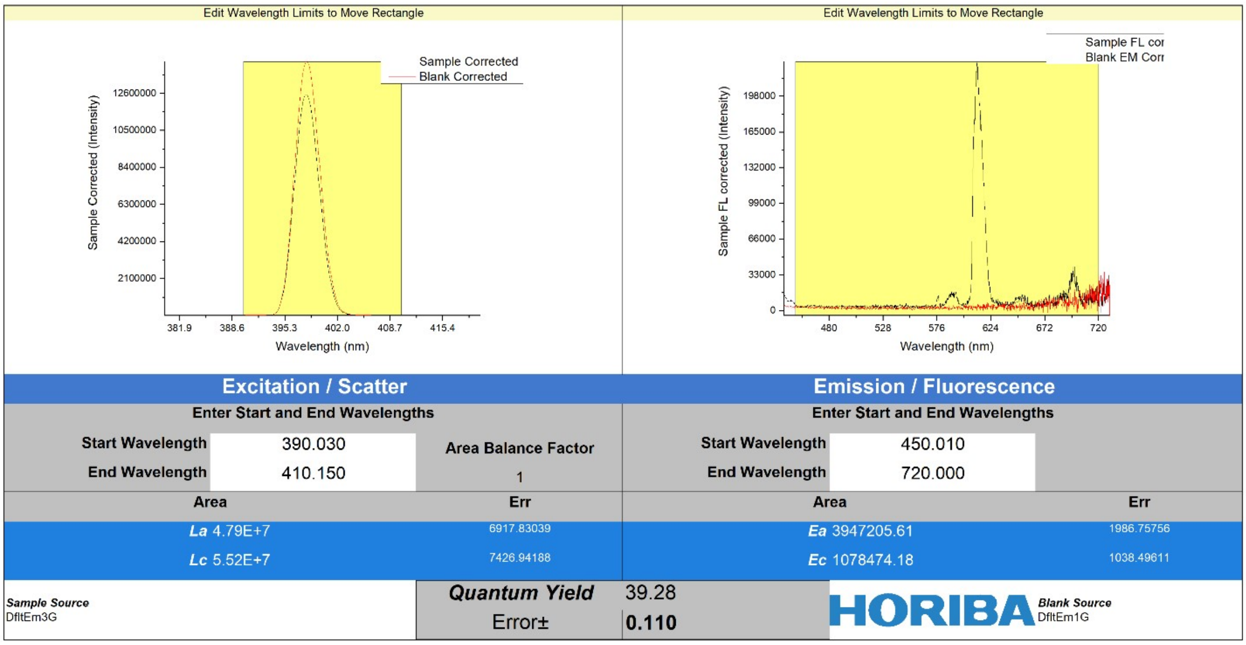

Figure S35. Absolute luminescence quantum yield measurements of PMMA encapsulated films of **3** (λ_{ex}=400)

Table S2. Photophysical properties of **1**–**3** (λ_{ex}= 400 nm and λ_{em} = 611 nm).

	τ_{Ln}(ms)[a]	τ_R (ms)[b]	Φ_{Ln} (%)[c]	Φ_{tot} (%)[d]	η_{sen} (%)[e]	k_r (s^{-1})[f]	k_{nr} (s^{-1})[g]
1	0.52	1.14	90	38	42	0.9×10^3	1.1×10^3
2	0.56	1.17	88	36	41	0.9×10^3	0.9×10^3
3	0.52	1.16	91	39	43	0.9×10^3	1.1×10^3

[a]Lanthanide luminescence lifetime obtained from TRPL spectra. [b]radiative lifetime τ_R, [c]the intrinsic luminescence quantum yield $\Phi_{Ln} = \tau_{Ln}/\tau_R$, [d]total luminescence quantum yields (Φ_{tot}), [e]sensitization efficiency $\eta_{sen} = \Phi_{tot} / \Phi_{Ln}$, [f]radiative decay rate constant $k_r = 1/\tau_R$ and [g]non-radiative decay rate constant, $k_{nr} = (\tau_R - \tau_{Ln}) / \tau_R \tau_{Ln}$.[2,3]

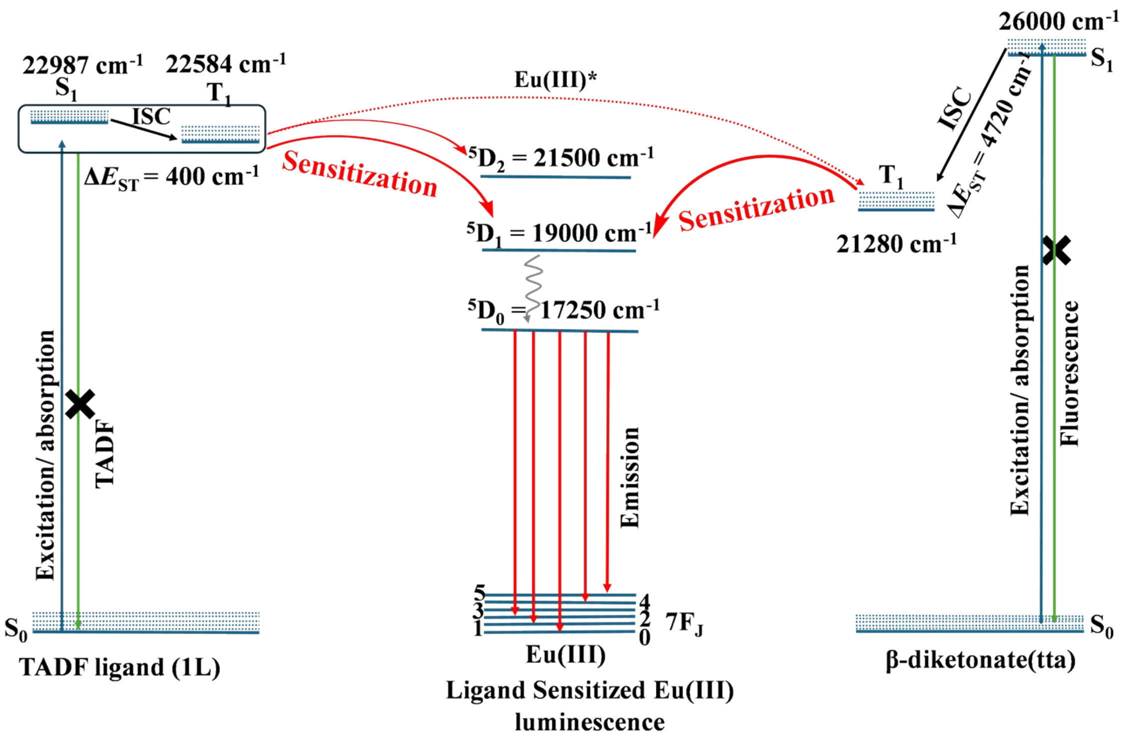

Figure S36. The mechanistic energy transfer pathways in the tta and TADF-ligand (**1L**) sensitized Eu(III) luminescence of coordination polymer **1** (energy levels are not up to the scale).

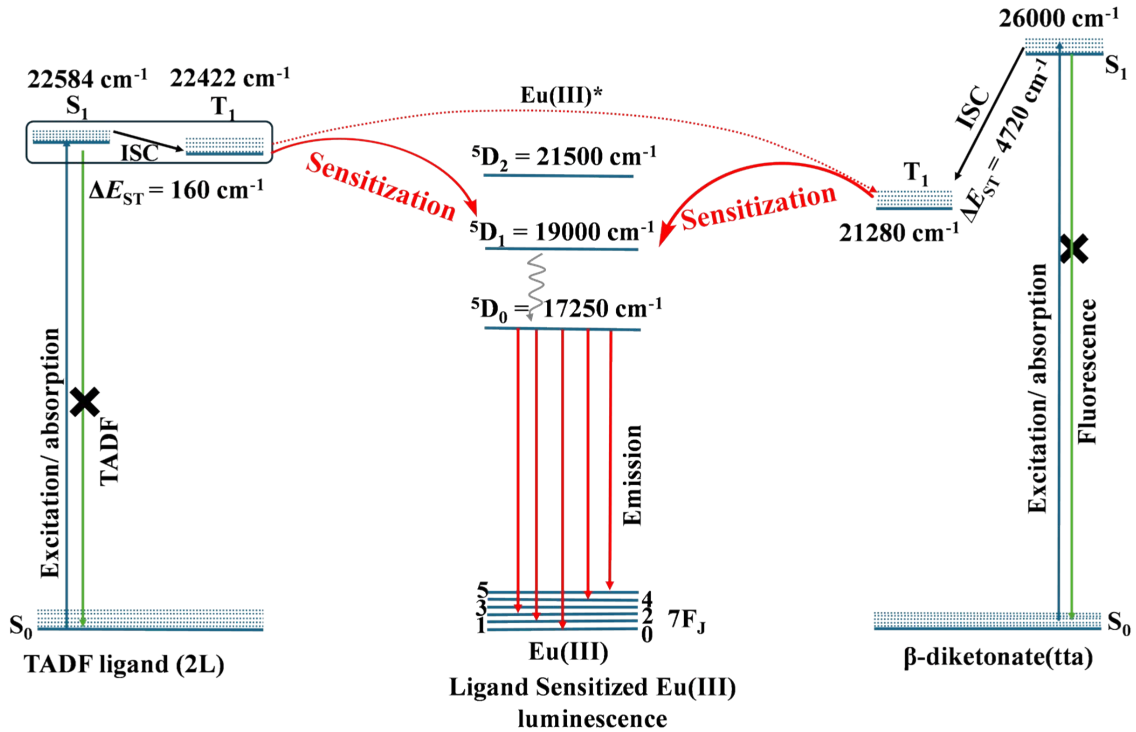

Figure S37. The mechanistic energy transfer pathways in the tta and TADF-ligand (**2L**) sensitized Eu(III) luminescence of coordination polymer **2** (energy levels are not up to the scale).

References

1 N. Sharma, M. Maciejczyk, D. Hall, W. Li, V. Liégeois, D. Beljonne, Y. Olivier, N. Robertson, I. D. W. Samuel and E. Zysman-Colman, Spiro-Based Thermally Activated Delayed Fluorescence Emitters with Reduced Nonradiative Decay for High-Quantum-Efficiency, Low-Roll-Off, Organic Light-Emitting Diodes, *ACS Appl. Mater. Interfaces*, 2021, **13**, 44628–44640.

2 Y. Kitagawa, M. Tsurui and Y. Hasegawa, Bright red emission with high color purity from Eu(iii) complexes with π-conjugated polycyclic aromatic ligands and their sensing applications, *RSC Adv.*, 2022, **12**, 810–821.

3 M. H. V Werts, R. T. F. Jukes and J. W. Verhoeven, The emission spectrum and the radiative lifetime of Eu3+ in luminescent lanthanide complexes, *Phys. Chem. Chem. Phys.*, 2002, **4**, 1542–1548.